X-ray Absorption Spectroscopy applied to Energy-related Materials

Valérie Briois

briois@synchrotron-soleil.fr

SOLEIL Synchrotron

Storage ring nominal energy: 2.75 GeV
(354 m de circumference)
Stored Current: 450 mA/500 mA

In operation since 2007

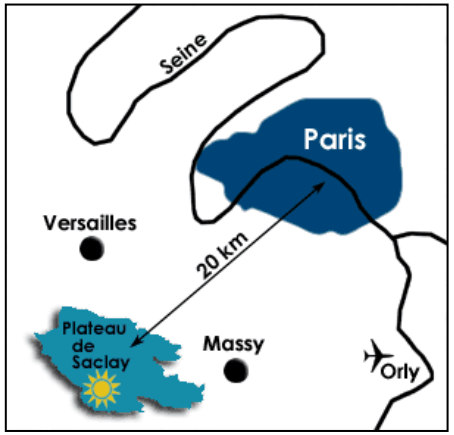

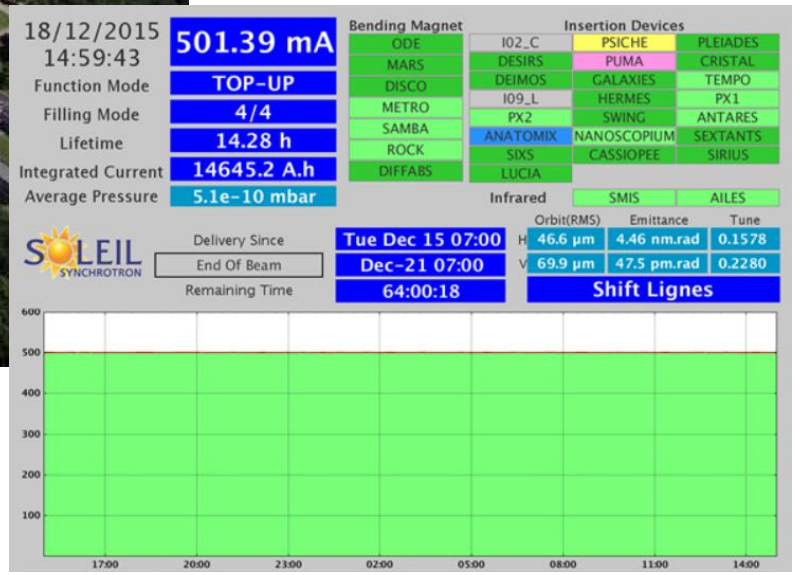

X-ray Absorption Spectroscopy applied to Energy-related Materials

Valérie Briois

briois@synchrotron-soleil.fr

Outline

1) XAS Introduction
2) ROCK: A Quick-EXAFS Beamline for Energy-related Materials
   - Sample Environment
   - Multivariate Analysis
3) From Quick-EXAFS to Full-Field Hyperspectral Quick-EXAFS Imaging

X –Ray Absorption Spectroscopy

$\mu x = \ln I_0 / I$ versus $h\upsilon$

Beer-Lambert law

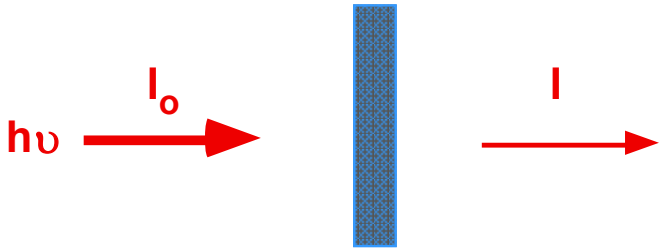

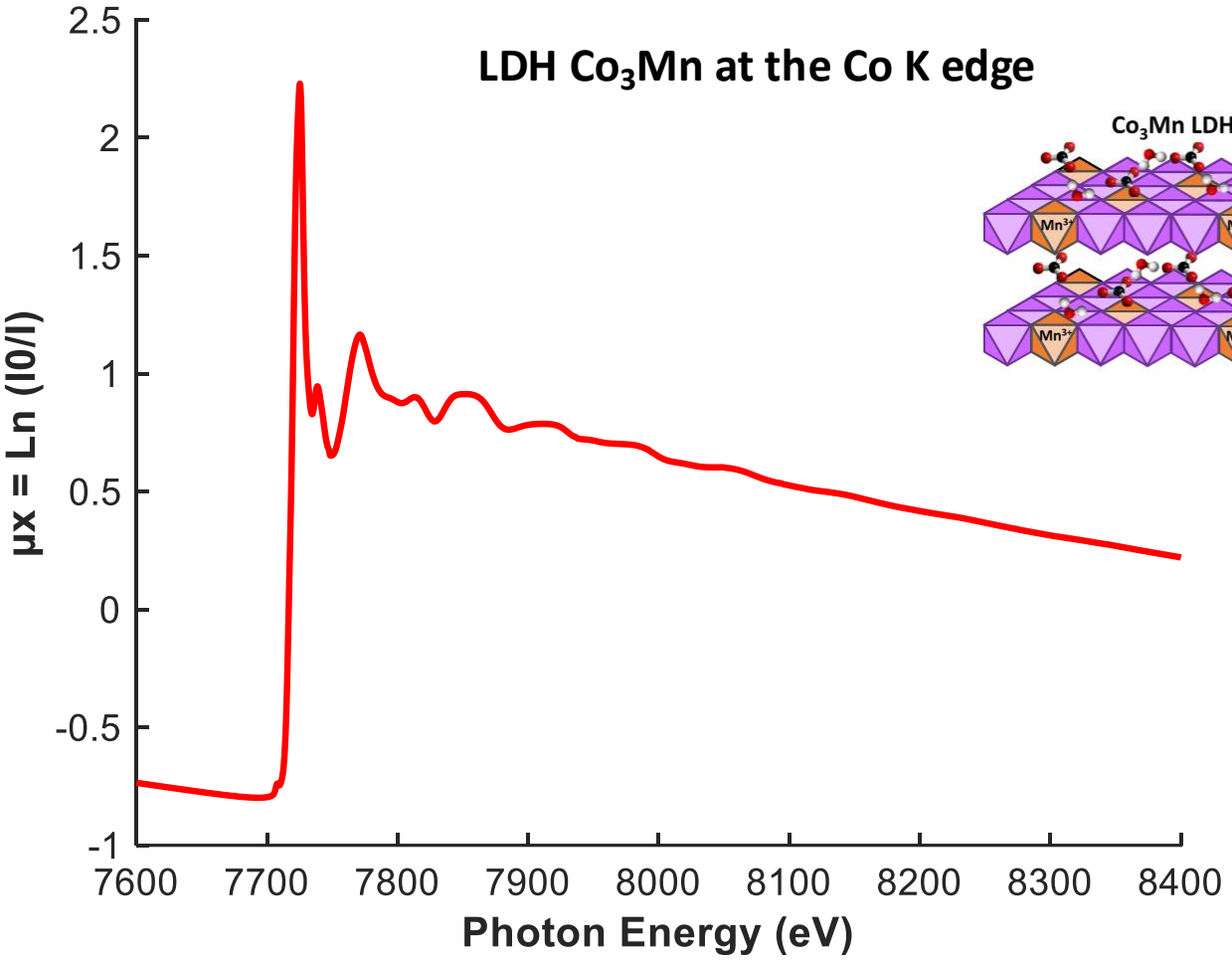

X –Ray Absorption Spectroscopy

$\mu x = Ln\ I_0/I$ versus $h\upsilon$

Beer-Lambert law

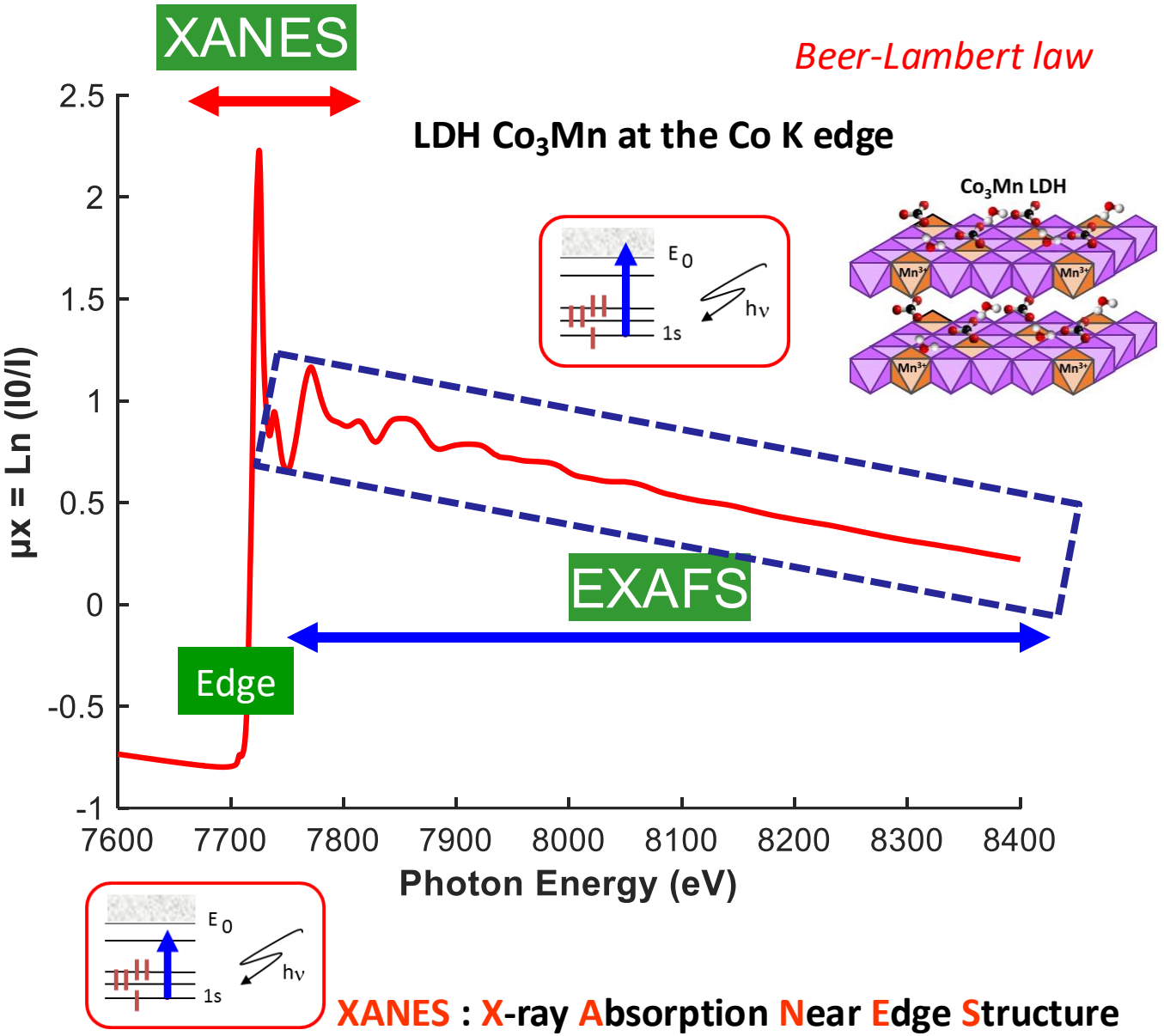

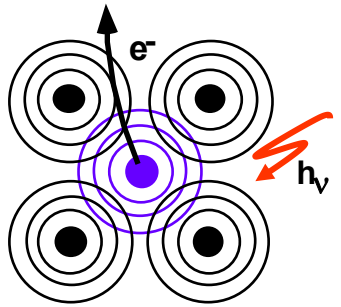

XAFS oscillations
Interferences between
Outgoing wave and
Backscattered waves

High-pressure EXAFS of solid and liquid Kr

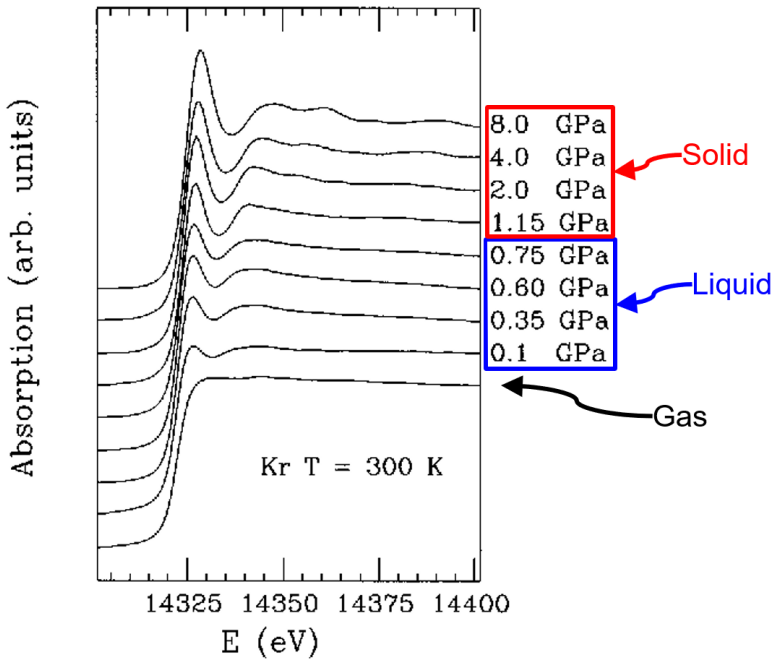

XANES : X-ray Absorption Near Edge Structure

EXAFS: Extended X-ray Absorption Fine Structures

A. Di Cicco, A. Filipponi, J. P. Itié and A. Polian, Phys. Rev. B 54 (1996) 9086-9098

EXAFS signal = Sum of damped sine waves, each being related to Contributions of neighbours around the absorbing atom at a given distance

EXAFS Formula : One-electron and single scattering

$$\chi(k) = -S_0^2 \sum_j \frac{N_j}{kR_j^2} \exp\left(\frac{-2R_j}{\lambda}\right) \exp\left(-2\sigma_j^2 k^2\right) A_j(\pi,k) \sin(2kR_j + \Phi_{a_j}(k))$$

Structural Parameters related to the j^{th} shell

N_j : Coordination number

R_j : Absorber-Neighbour Distance

σ_j : Debye-Waller Factor

Atom … **on**

$A_j(\pi,$ … **rir** … **r j**

Φa_j **k** … **ph**

λ : **El** … **ctr** … **Path**

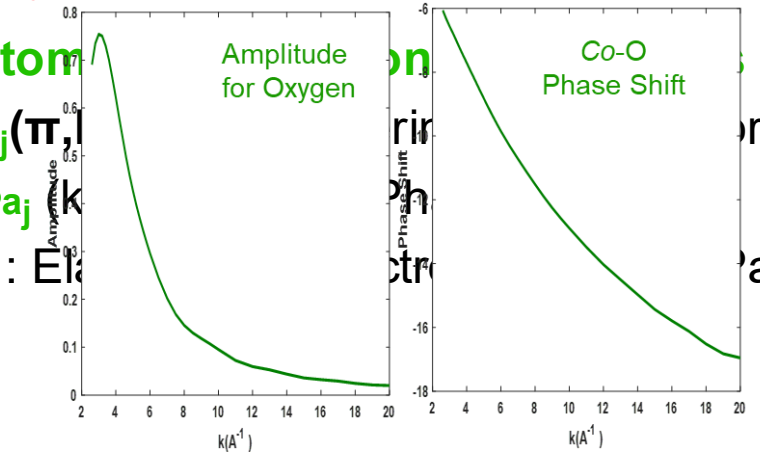

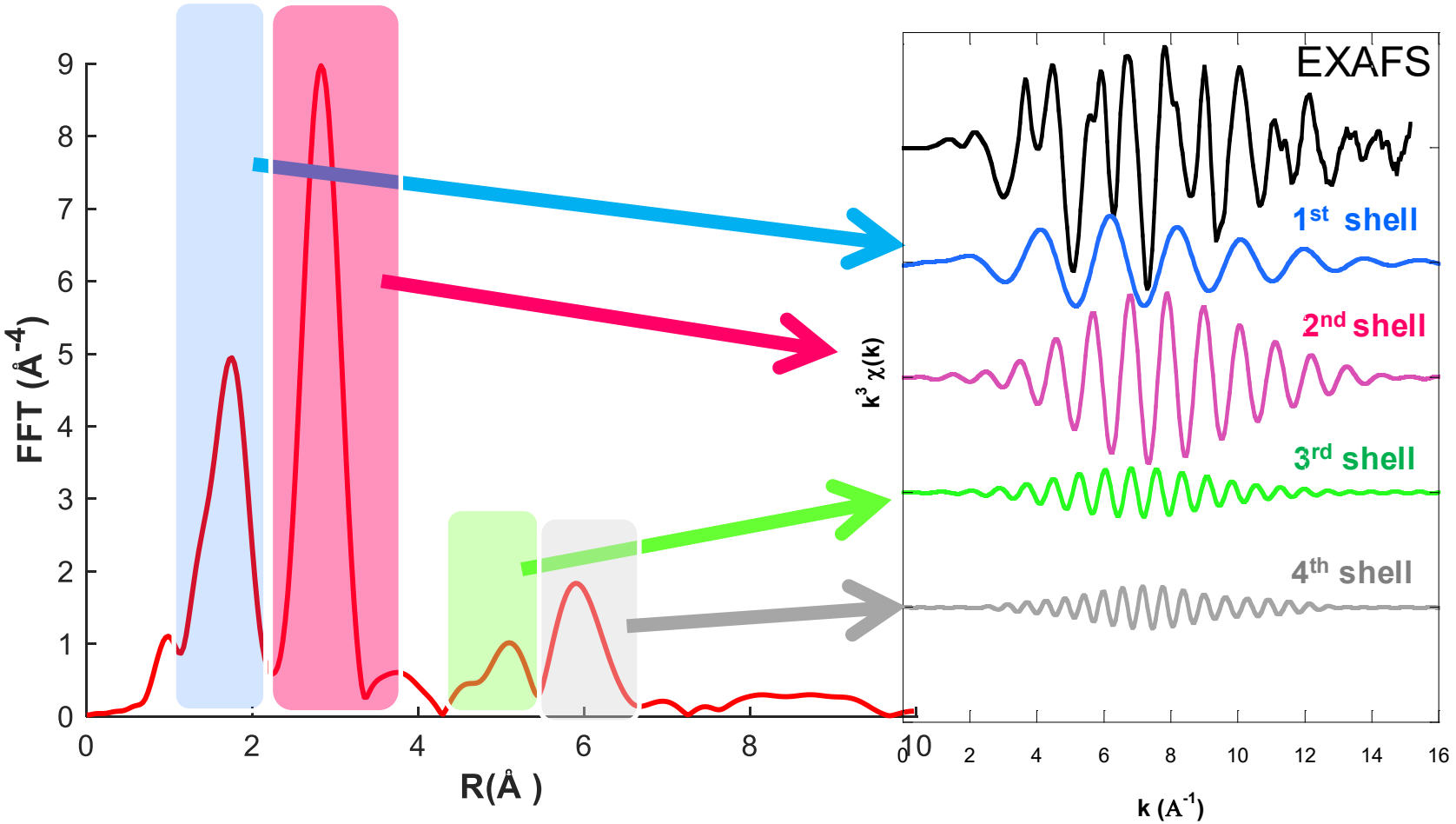

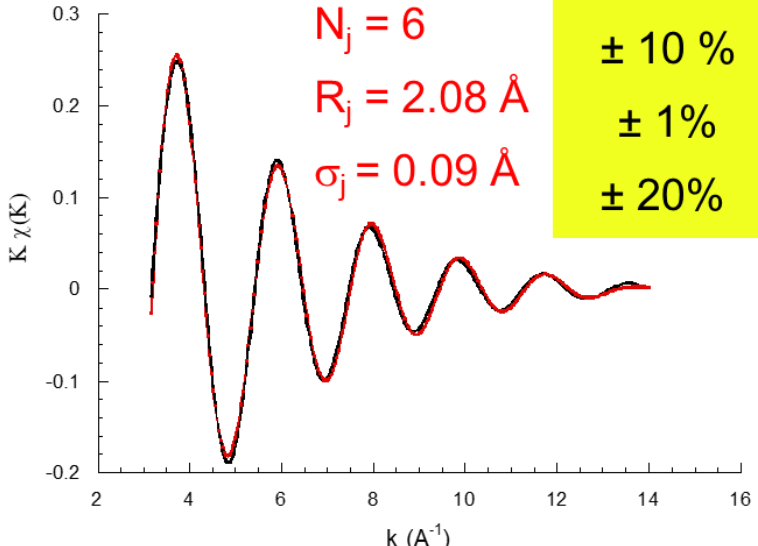

Accuracy

± 10 %

± 1%

± 20%

A few words about the XANES

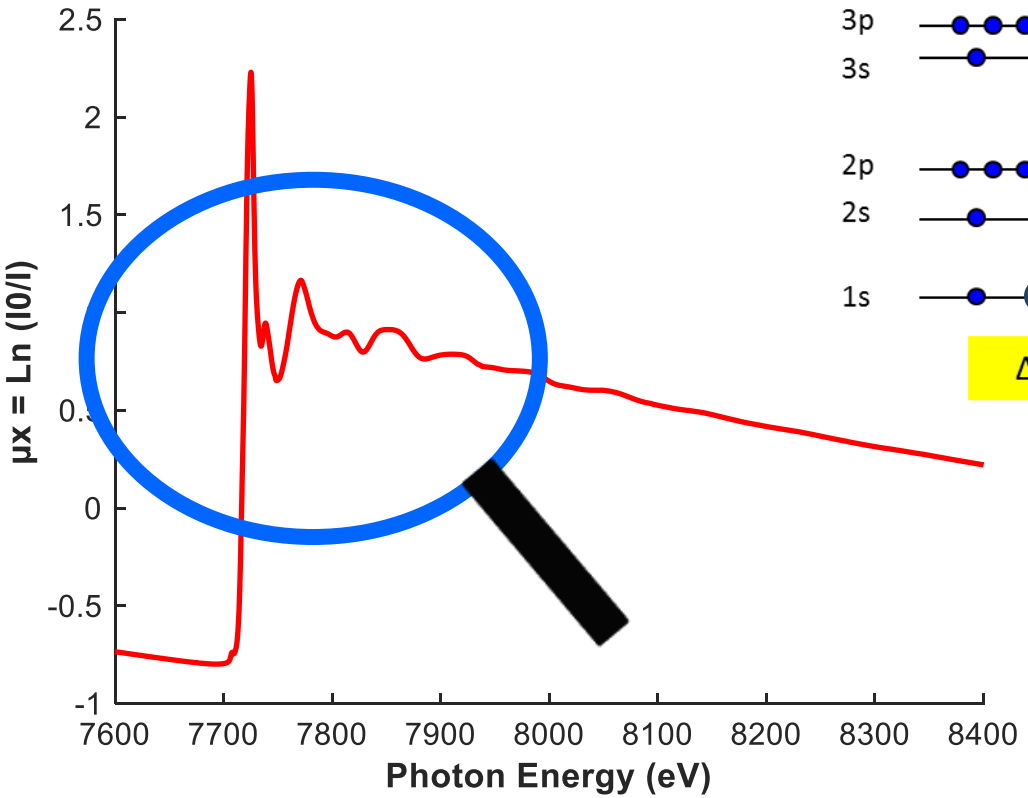

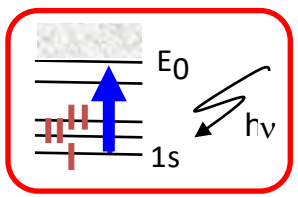

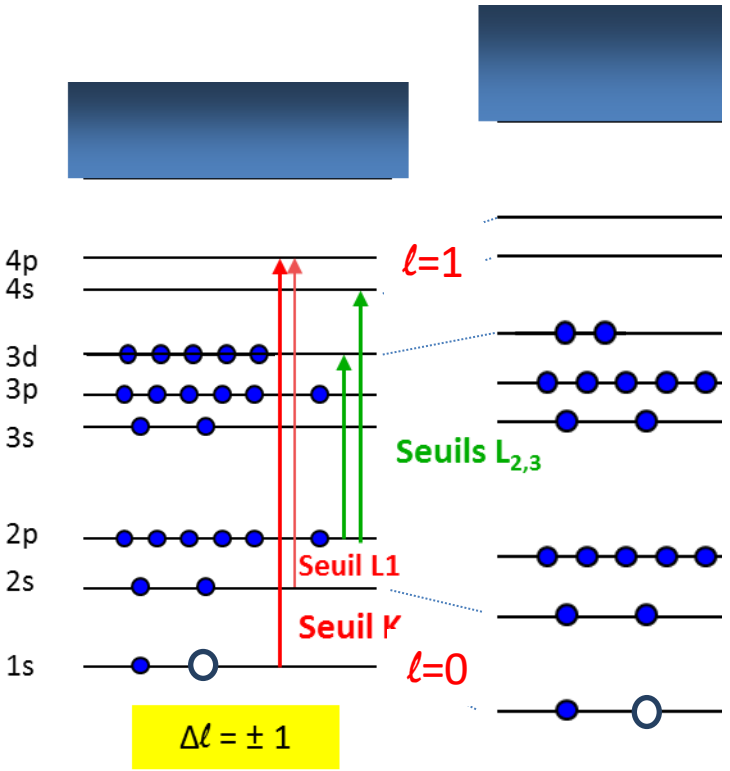

OXIDATION

d-p hybridization

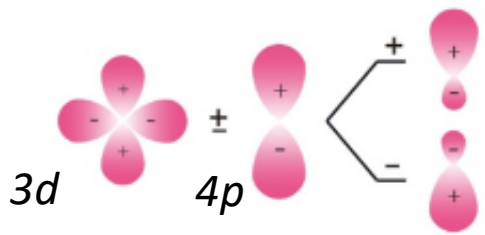

Non-Centrosymmetric Group

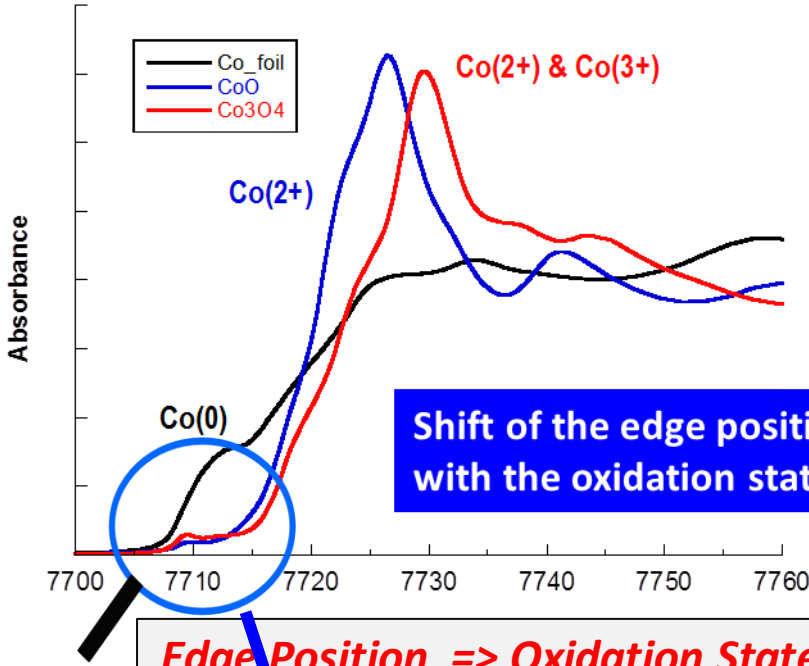

Shift of the edge position with the oxidation state

Edge Position => Oxidation State

M. Hunault et al. J. Phys.: Conf. Series 712 (2016) 012005

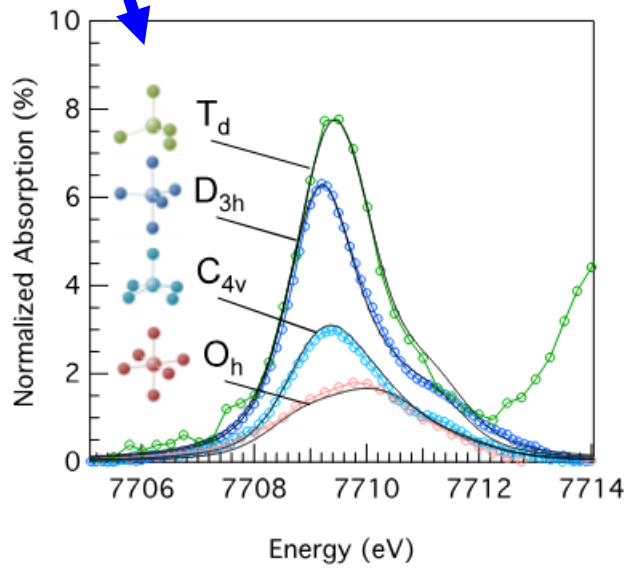

Intensity of Pre-Edge => Symmetry

X-ray Absorption Study of Battery Electrodes

X-ray Absorption Spectroscopy is an element-selective technique providing powerful information on :

- the local order around the absorbing atom (distance, N, Ligand…)
- oxidation state
- local point group symmetry

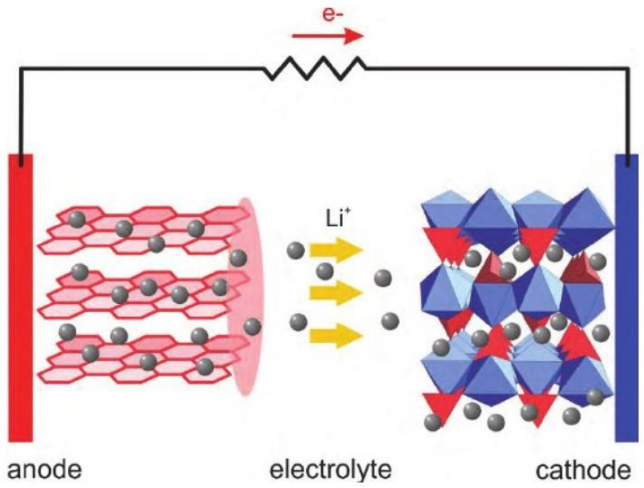

DOI: 10.5772/21635

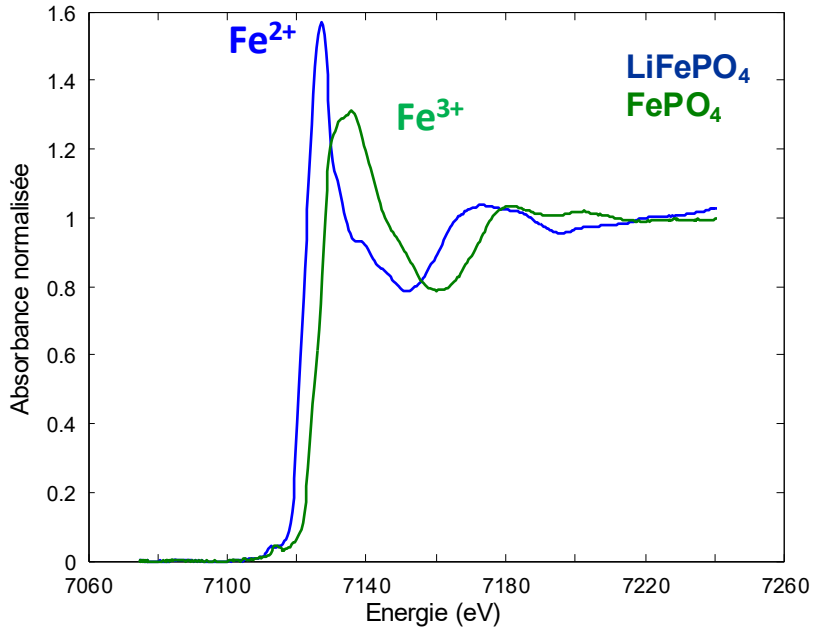

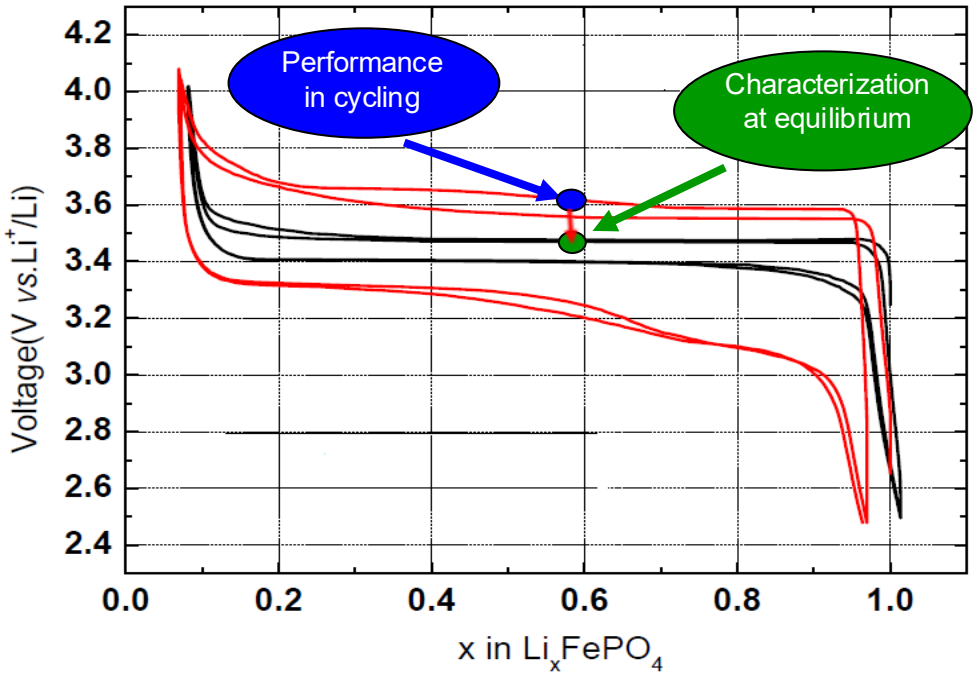

https://www.researchgate.net/publication/221913605_Composite_Cathode_Material_for_Li-Ion_Batteries_Based_on_LiFePO4_System

Operando XAS Measurements are mandatory

Characteristics of the ROCK beamline

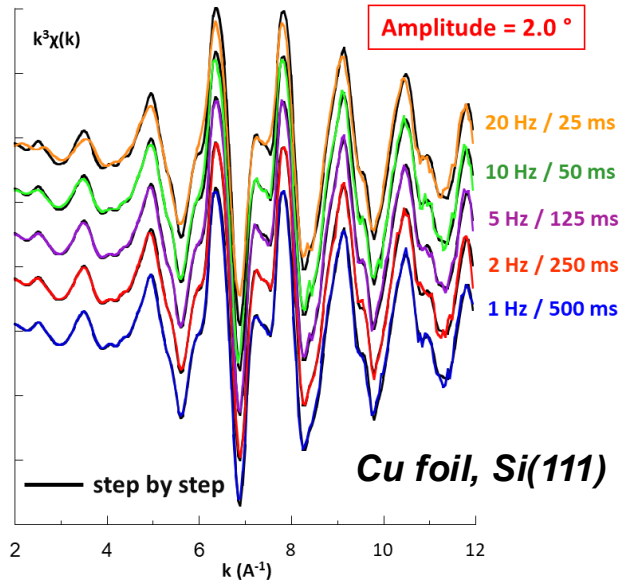

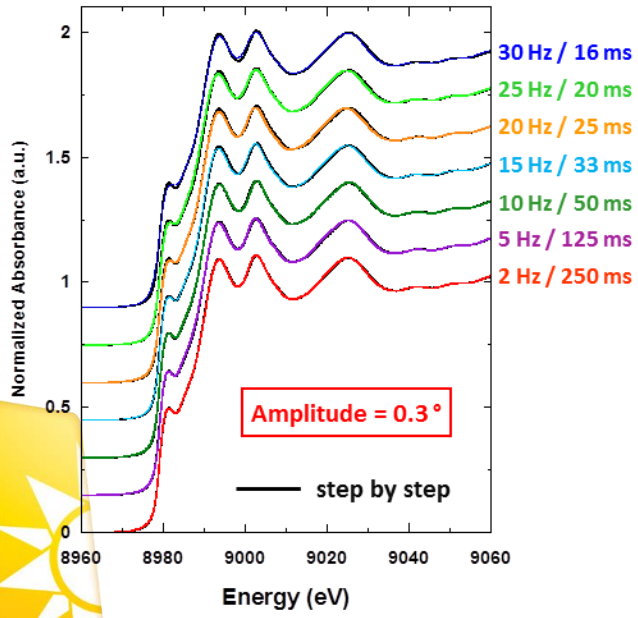

1 LN_2-cooled monochromator

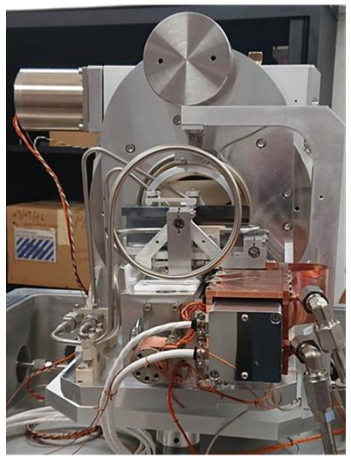

Si(220)
6 - 43 keV

2 water-cooled monochromators

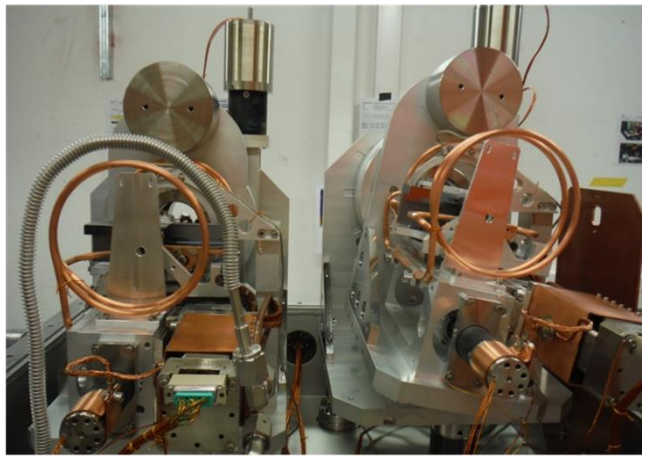

Si(111)
4 - 26 keV

Si(111)
4 - 21 keV

Source:	**2.81 T Super Bend**
Energy Range:	**4 – 42 keV**
Flux @ 8.5 keV:	**Si(111) : 1.7 10^{12} ph/s**
Flux @ 20 keV:	**Si(111) : 1.0 10^{12} ph/s**
Flux @ 20 keV:	**Si(220) : 5.0 10^{11} ph/s**
Flux @ 35 keV:	**Si(220) : 1.5 10^{11} ph/s**
Time resolution in the ms range	

Briois et al., J. Phys.: Conf. Ser. 712 (2016) 012149

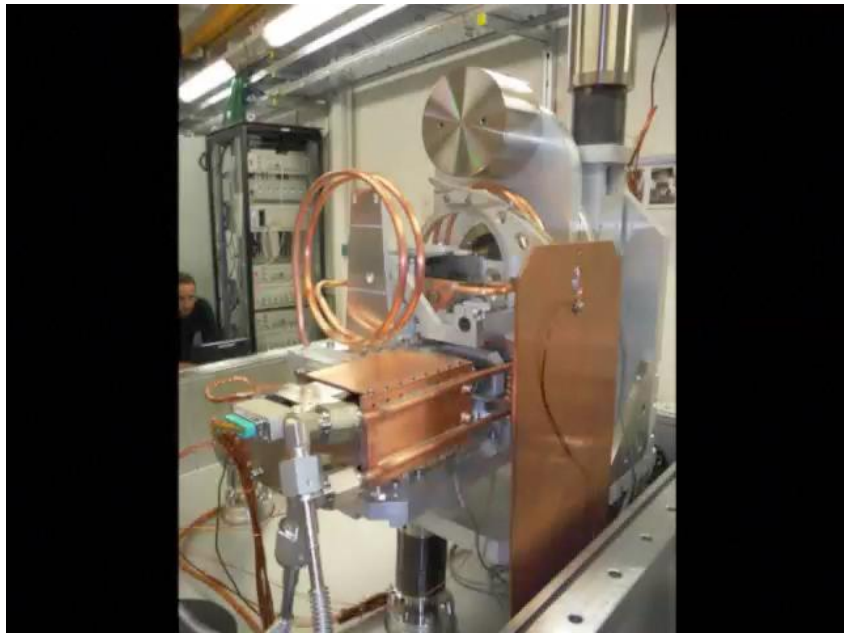

Oscillation frequency : 0.1 Hz to 30 Hz
for one spectrum => 16 ms to 5s

Oscillation amplitude range: 0.3 to 3.9°
- at least 1000 eV spectra (EXAFS)

Characteristics of the ROCK beamline

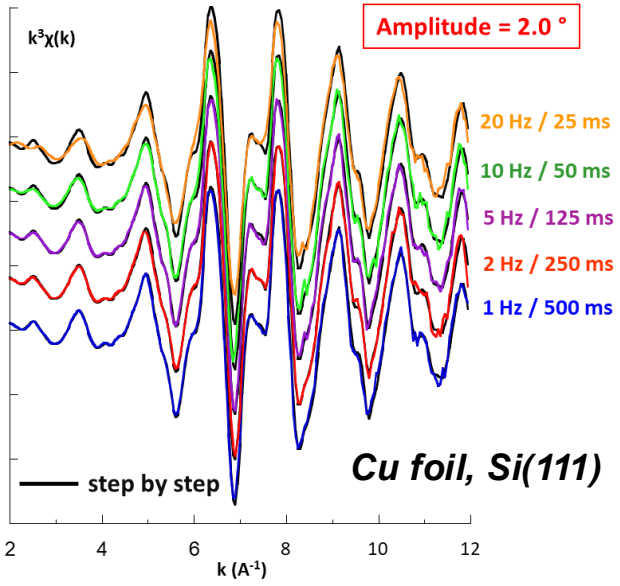

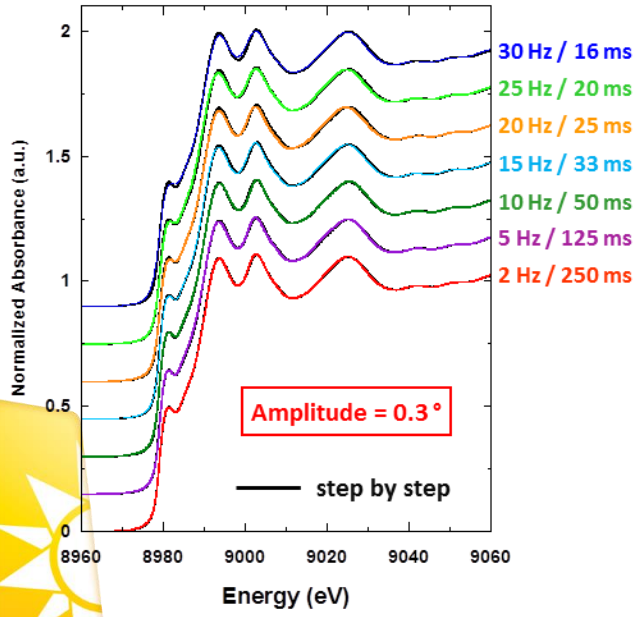

1 LN_2-cooled monochromator

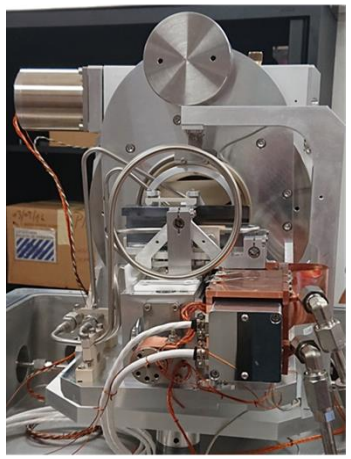

Si(220)
6 - 43 keV

2 water-cooled monochromators

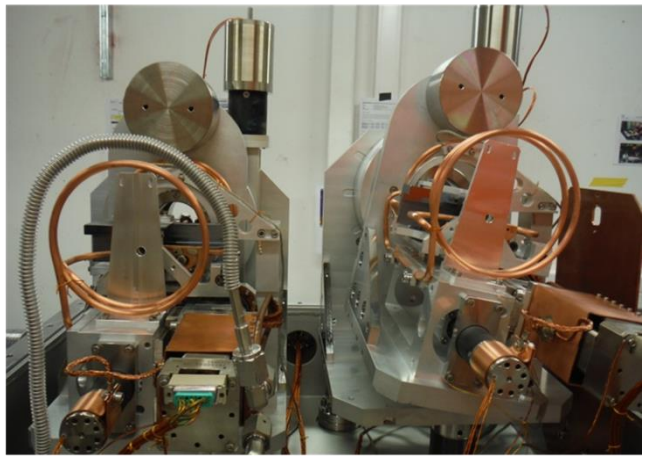

Si(111)
4 - 26 keV

Si(111)
4 - 21 keV

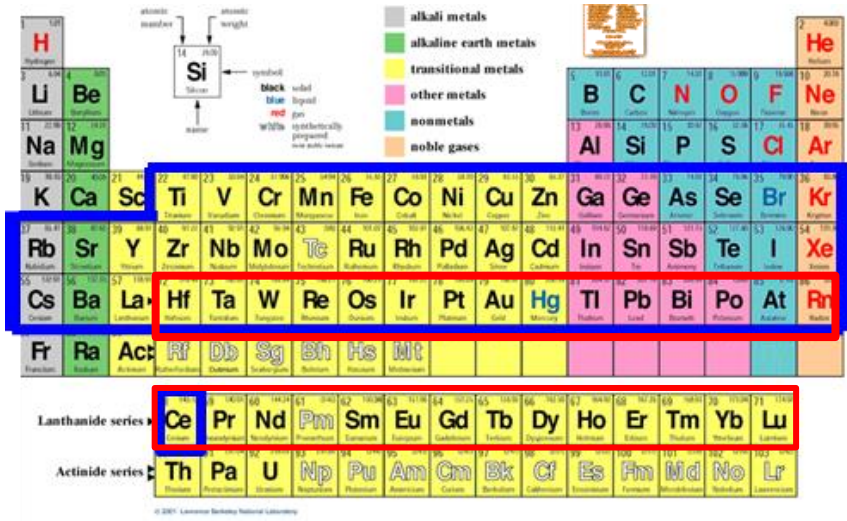

65 elements can be measured …

Source:	**2.81 T Super Bend**
Energy Range:	**4 – 42 keV**
Flux @ 8.5 keV:	**Si(111) : 1.7 10^{12} ph/s**
Flux @ 20 keV:	**Si(111) : 1.0 10^{12} ph/s**
Flux @ 20 keV:	**Si(220) : 5.0 10^{11} ph/s**
Flux @ 35 keV:	**Si(220) : 1.5 10^{11} ph/s**
Time resolution in the ms range	

Briois et al., J. Phys.: Conf. Ser. 712 (2016) 012149

Science

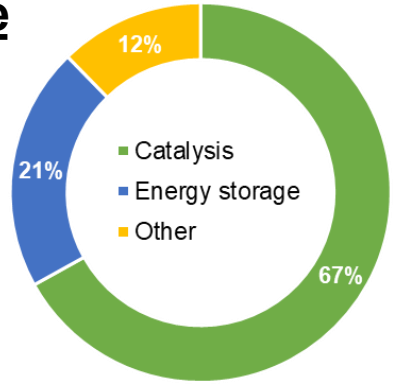

Dedicated sample environments for Energy Storage

Half Cell Geometry

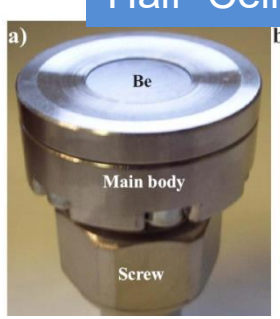

JES, 157, (2010) A606-A610

Multi-electrochemical cells

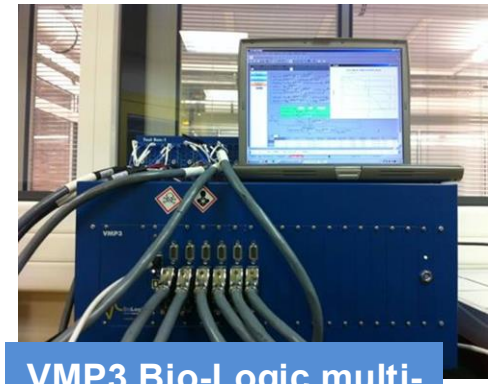

VMP3 Bio-Logic multi-channel potentiostat

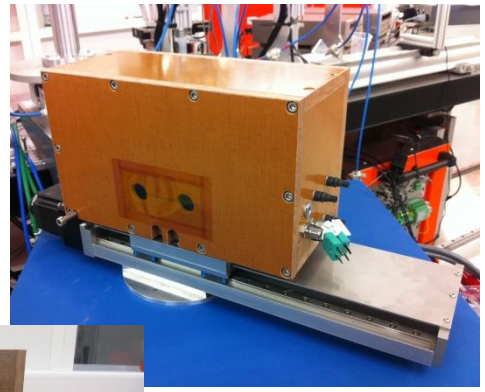

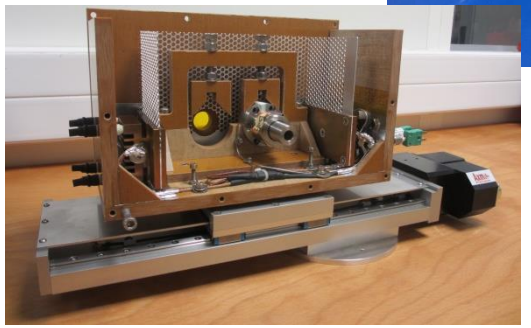

Thermostated box for electrochemical cells

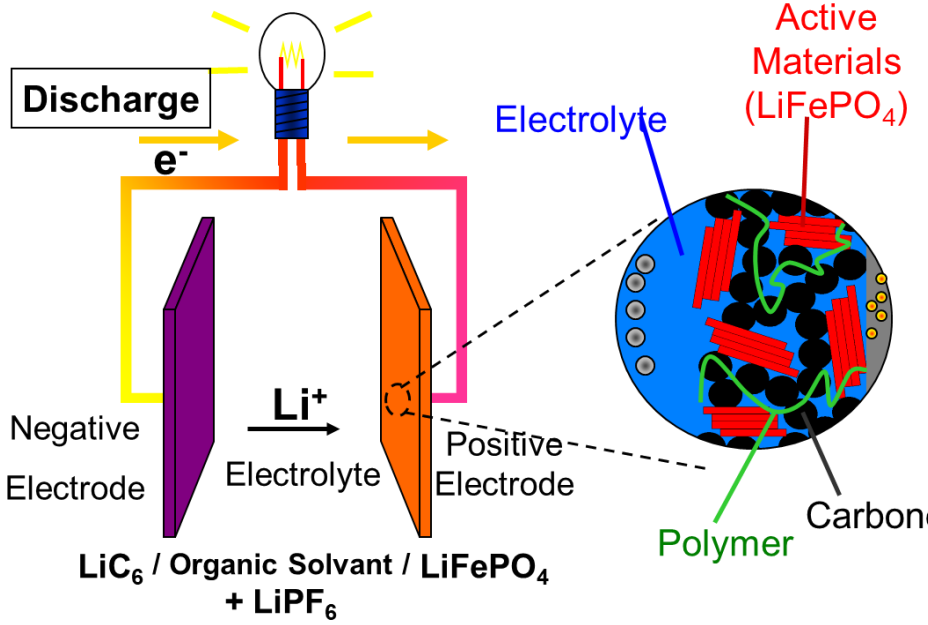

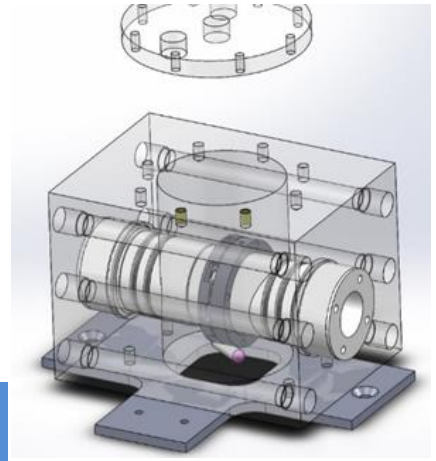

Electrochemical cell

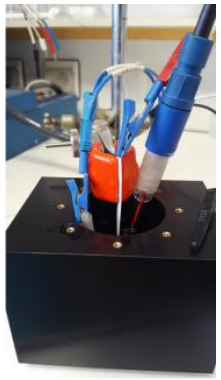

Super-Capacitors

Li-Battery
Na-Battery
Mg-Battery

Dedicated sample environments for Energy Conversion

Electrocatalysis

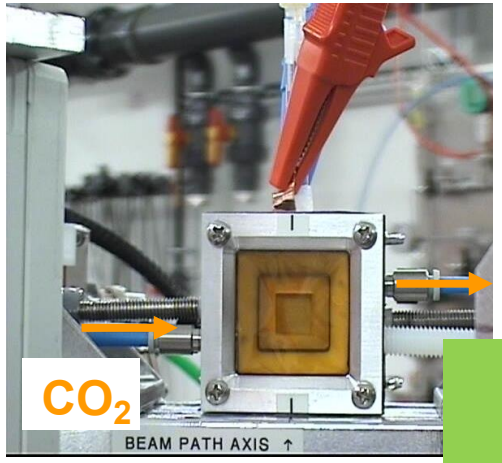

Photo-catalysis

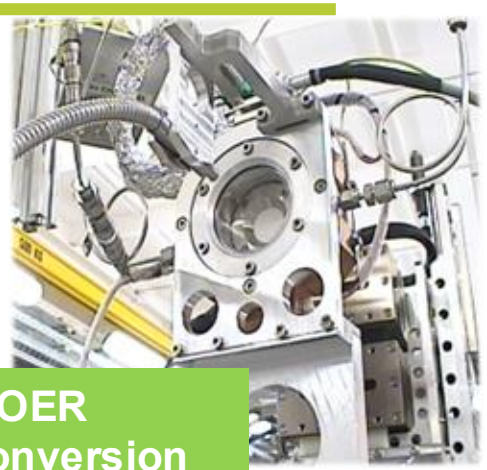

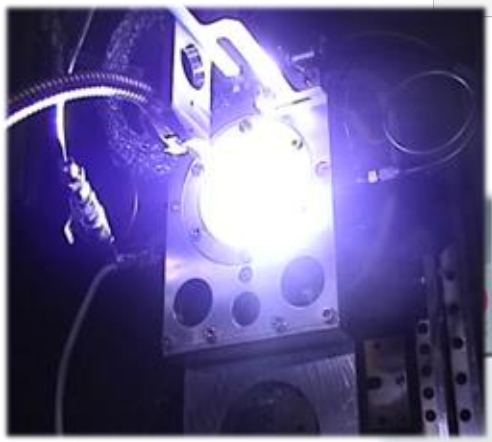

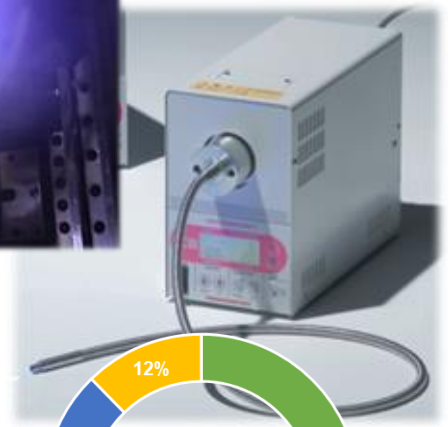

HER & OER
CO_2 photoconversion
Ethanol photoconversion

Thermal Catalysis

(a) Lytle-type cells

1 bar, RT – 600°C

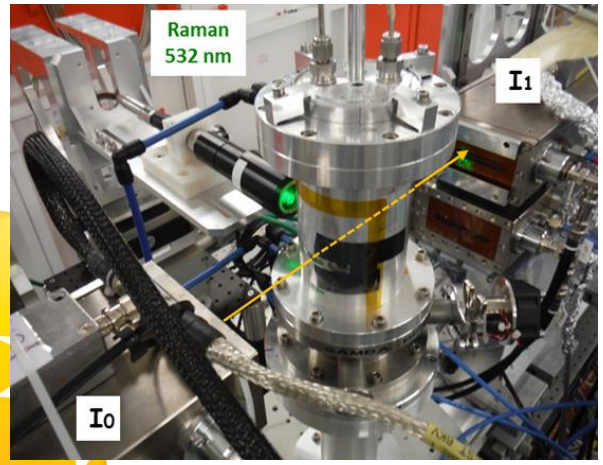

(b) Capillary cells

20 bar, RT – 1000°C

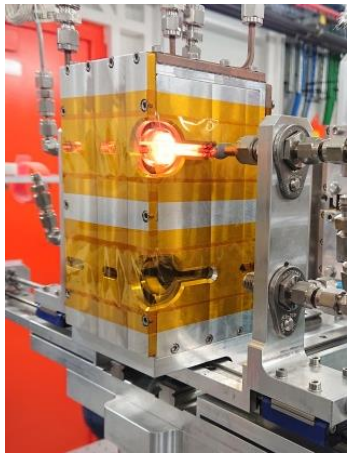

(c) Gas delivery systems

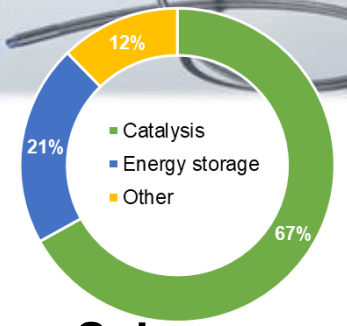

Science

Ethanol Steam Reforming
Dry Methane reforming
Fischer Tropsch
HDS & HDO
CO_2 – CO hydrogenation
Chemical Looping
Combustion

Detection Modes for XAS

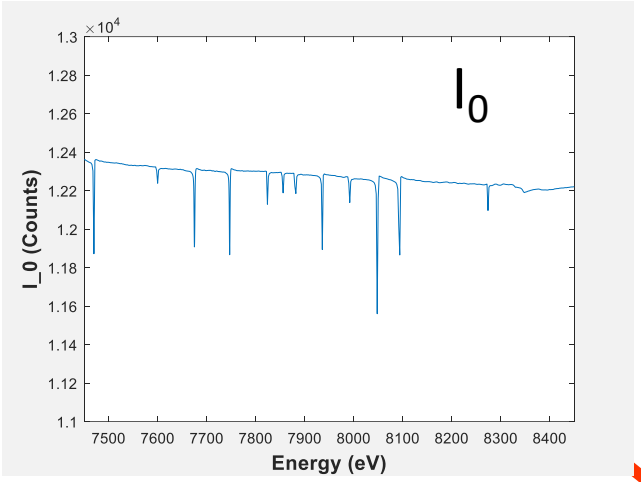

Transmission Mode

Concentrated Systems

I_o → | → I

$\mu x = Ln(I_0/I)$

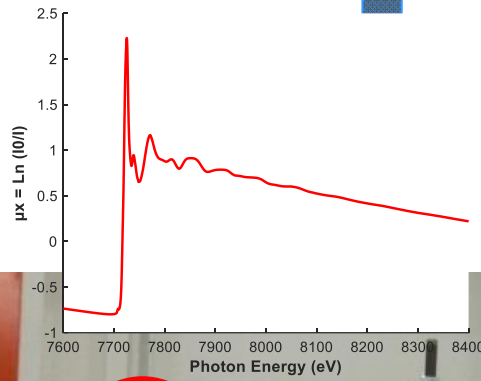

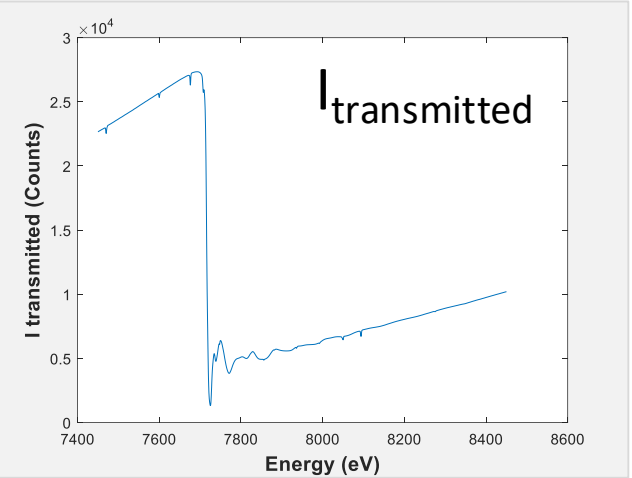

$\mu x = Ln\ I_0/I$ versus $h\upsilon$

Beer-Lambert Law

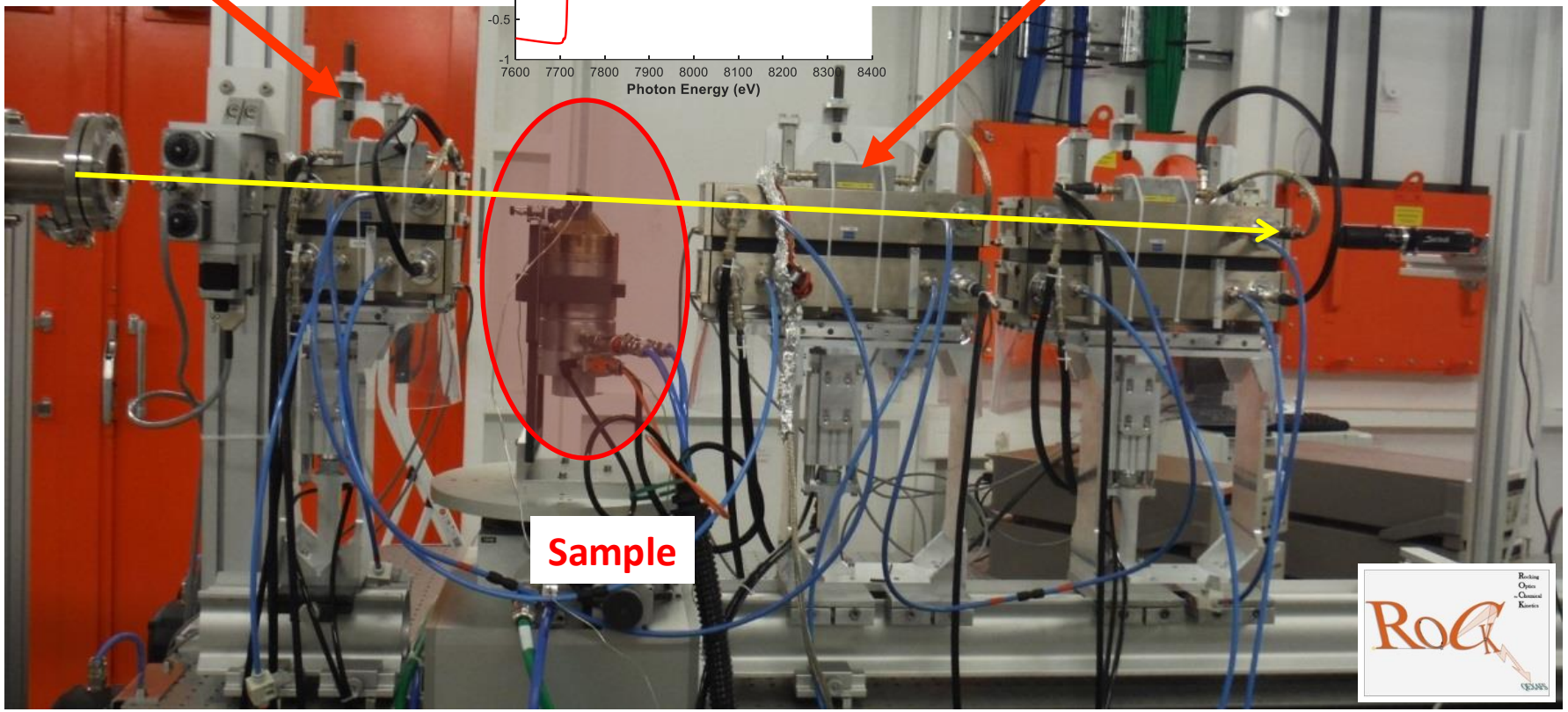

Operando XAS study on LNO with a new electrochemical cell on ROCK beamline

G. Moëhl, L. Pérez Ramirez, A. Iadecola and S. Belin.

New cell design :
Gilles Moëhl & Laurent Barthe

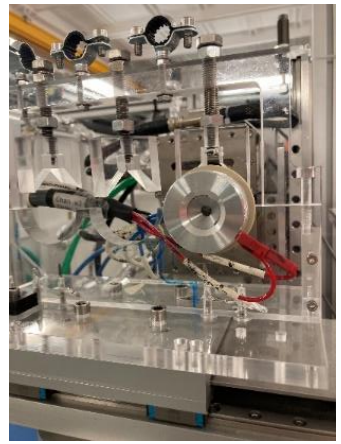

- Diamond peek-mak: LNO BASF/Celgard/Lithium, 28µL LP57 electrolyte, 4.5 bar pressure
- C=225 mAh 3-4.3 V vs lithium 2 cycles at C/10 + 2 cycles at C/4
- Speed 2Hz (250ms) 2 positions recorded, average time = 2min

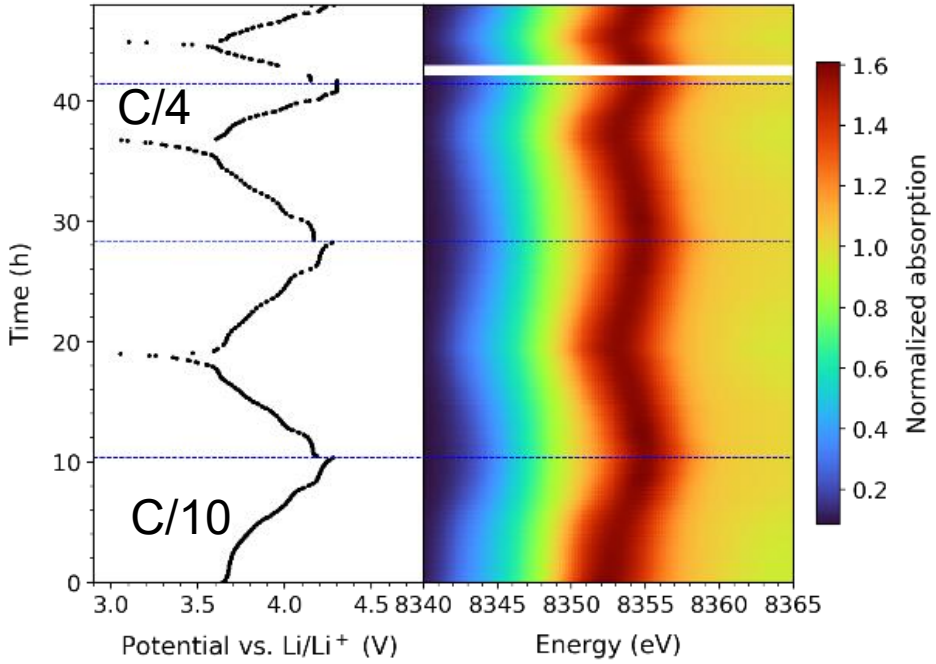

Galvanostatic Cycling curve

229 Ni K-edge XAS spectra

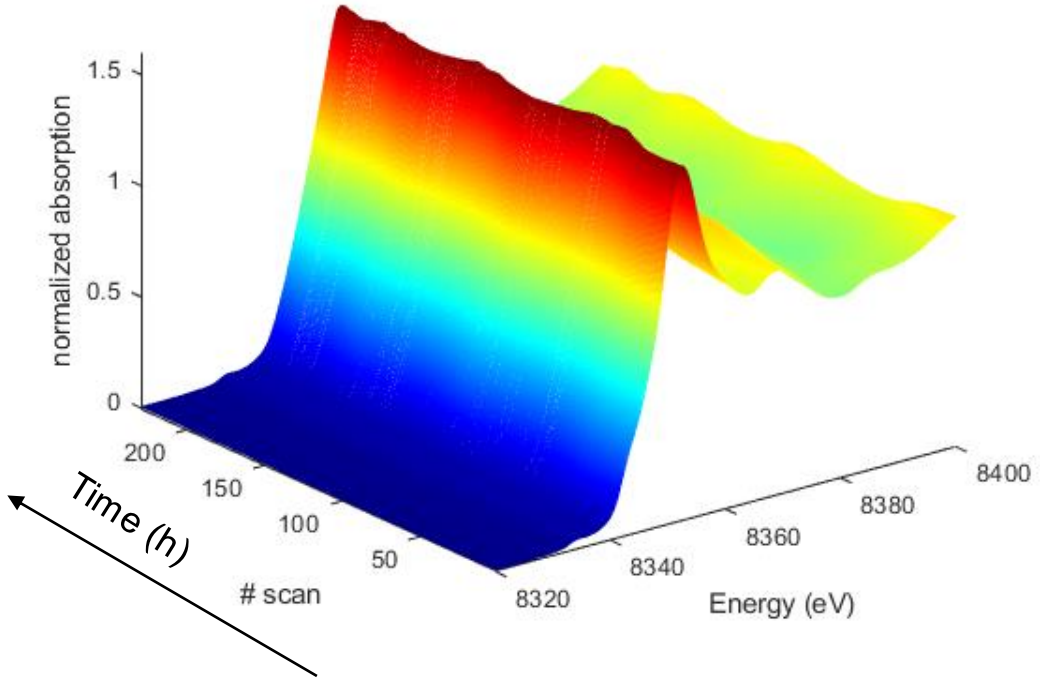

Quick-EXAFS : a lot of XAS data to analyze

Multivariate Curve Resolution
Alternating Least Squares Fitting

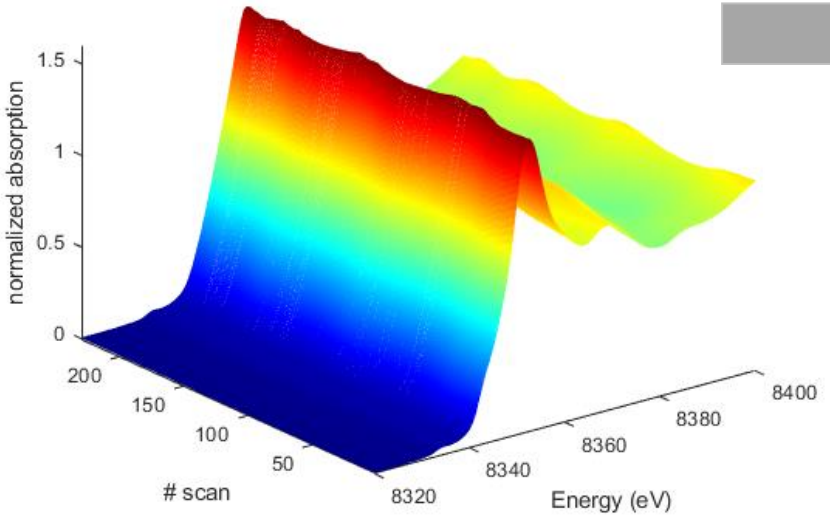

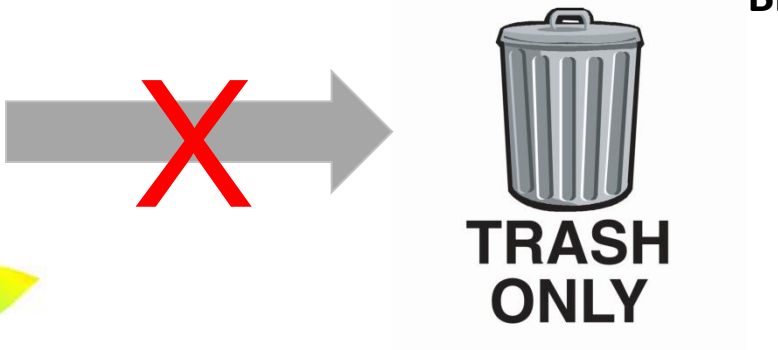

Bilinear Decomposition is fully verified for XAS
(Beer-Lambert Law Abs = $\Sigma C_i Abs_i$)

MCR-ALS

$$D = CS^T + E$$

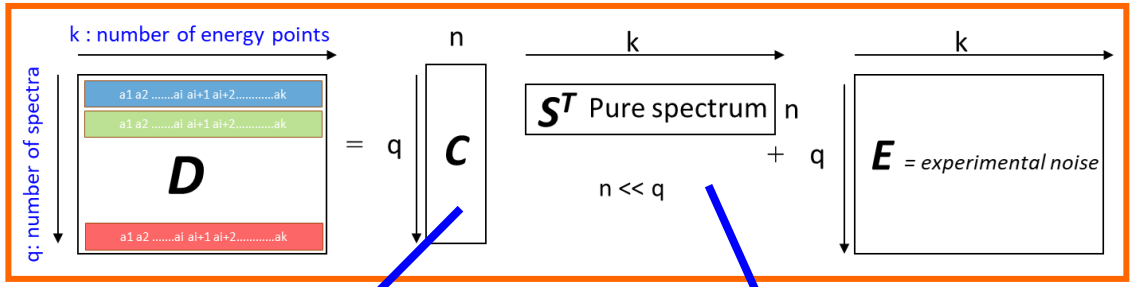

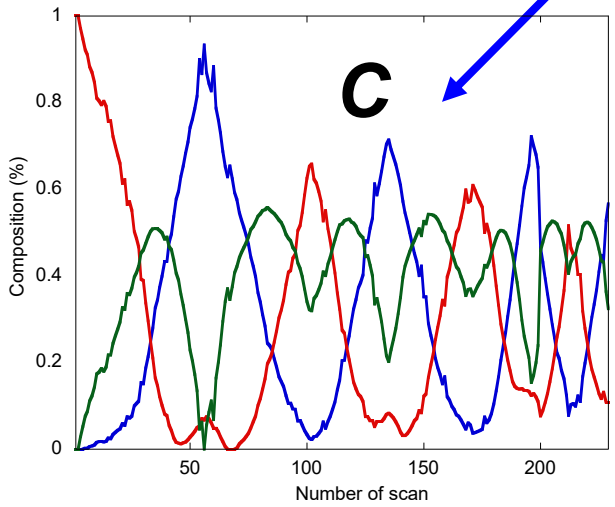

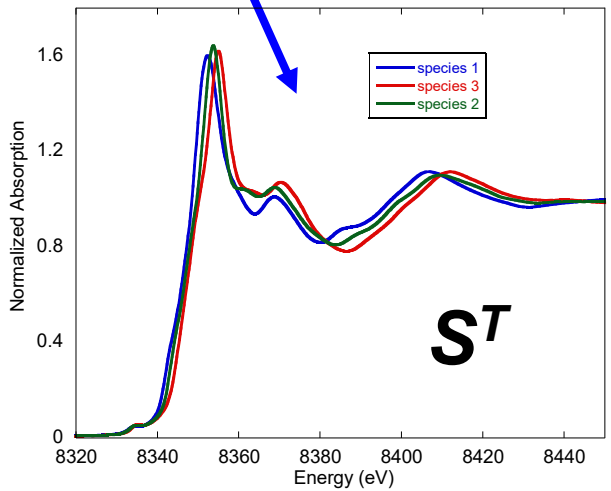

Matlab toolbox
R. Tauler et al. Chemom. Intell.Lab. Syst. (2015) 140, 1

Applications for XAS:
Catalysis Today (2014) 229, 114-122
Comptes Rendus Chimie (2016) 19, 1337-1351
J. Phys. Chem. C (2017) 121, 18544-18556
Catalysis Today (2019) 336, 63-73
PCCP (2020) 22, 18835-18848
Rad. Phys. Chem. (2026)

Multivariate Curve Resolution with Alternating Least Squares Fitting

MCR-ALS : How does it work ?

$$D = CS^T + E$$

Initial estimate of S^T

i.e. Guess of 3 spectra

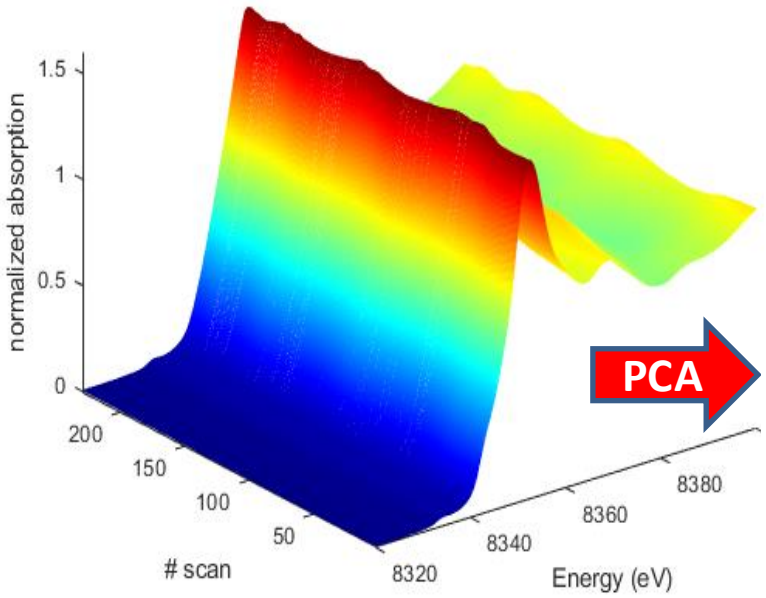

PCA

Estimation of number of Components
e.g. 3 components
SIMPLISMA, EFA

ALS minimization

$$\min ||D - CS^T||^2$$

Determination of concentration matrix C
which is used as a new guess for the minimization

Iteration is stopped when convergence is achieved.

CONSTRAINTS to help CONVERGENCE of MCR-ALS fitting

- Non-negativity of C and S

- Closure relation for the concentration of the n components:

$$\sum_{i=1}^{n} C_i = 100\ \%$$

- Unimodality of concentration profiles

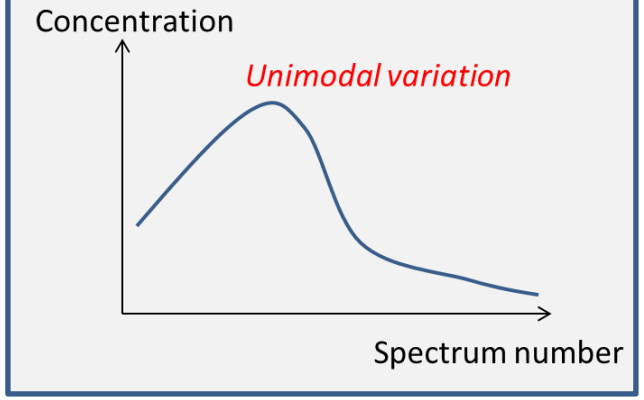

Operando XAS study on LNO with a new electrochemical cell on ROCK beamline

G. Moëhl, L. Pérez Ramirez, A. Iadecola and S. Belin.

New cell design :
Gilles Moëhl & Laurent Barthe

BIG-MAP

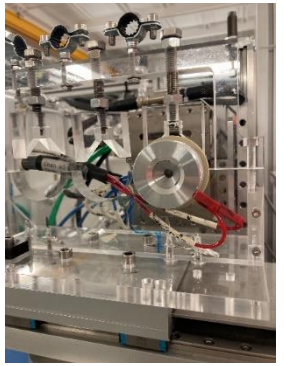

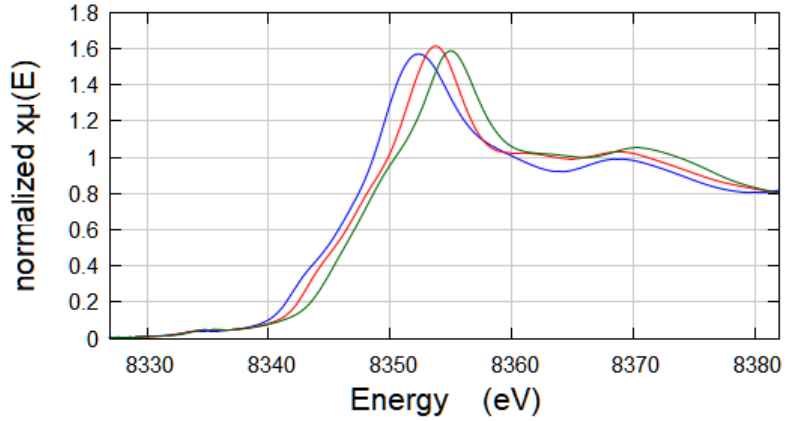

Concentration profiles vs. Potential

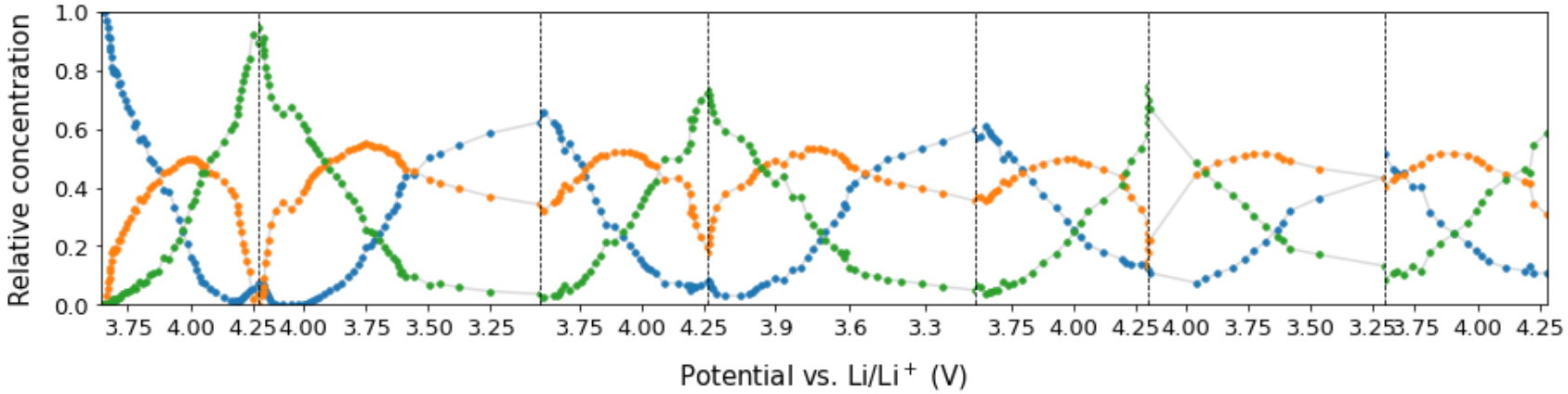

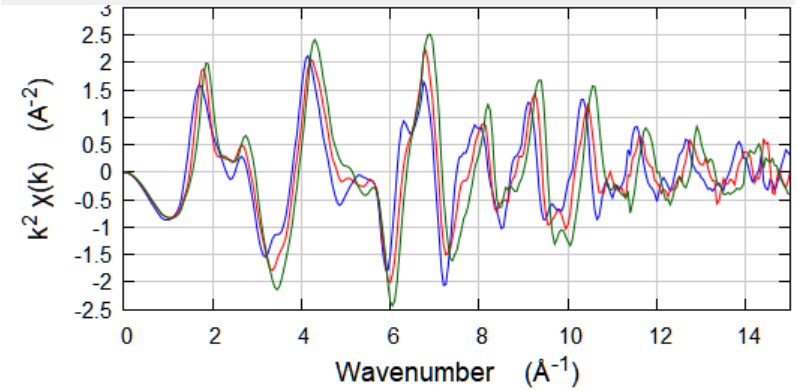

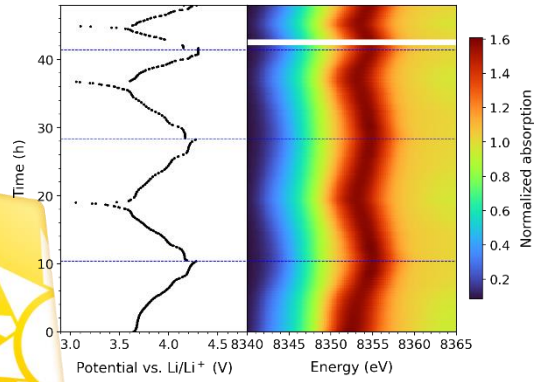

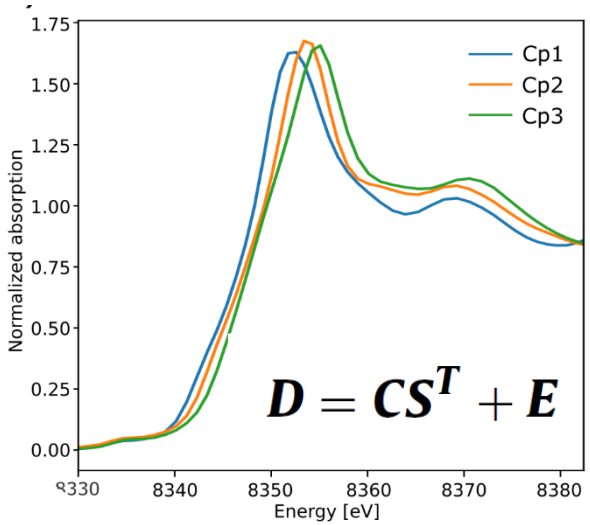

Phase Identification
⇒ fit of the EXAFS spectra of the 3 Cps instead of 229 spectra

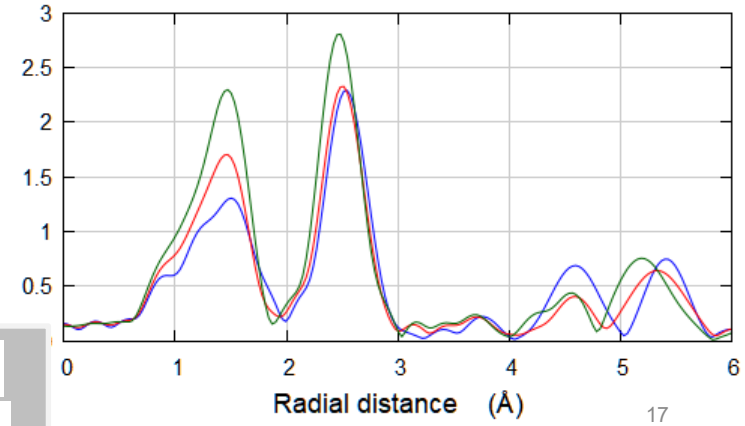

Adv. Energy Mater. **2024**, *14*, 2401413

J. Mater. Chem. A, 2025, **13**, 28305-28317

Full Field Hyperspectral Imaging at ROCK

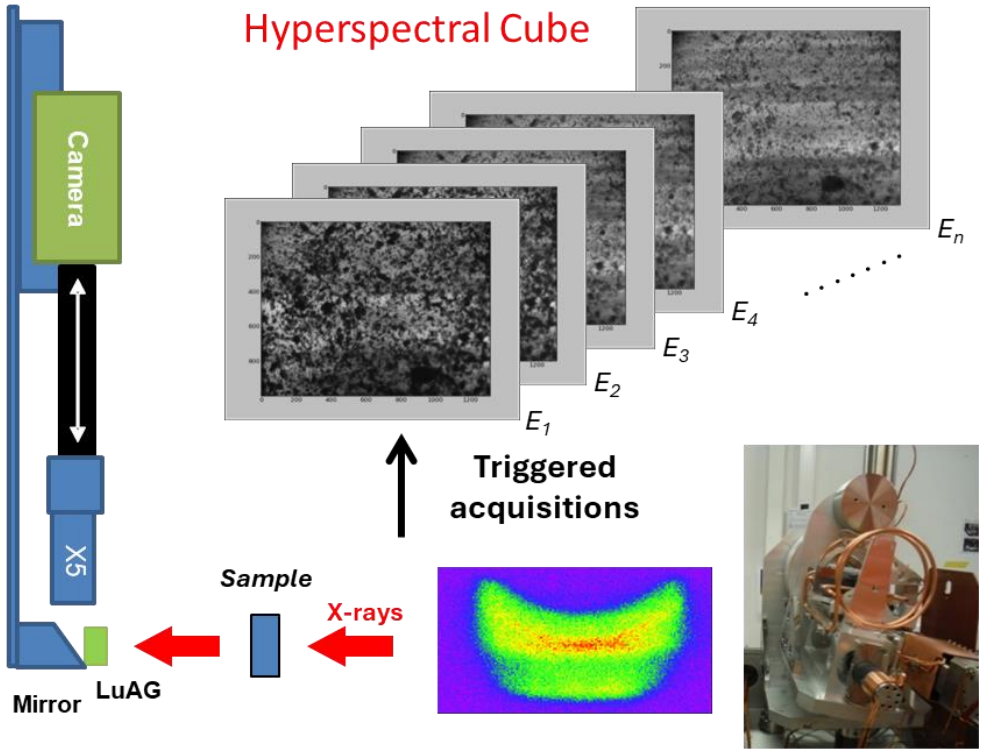

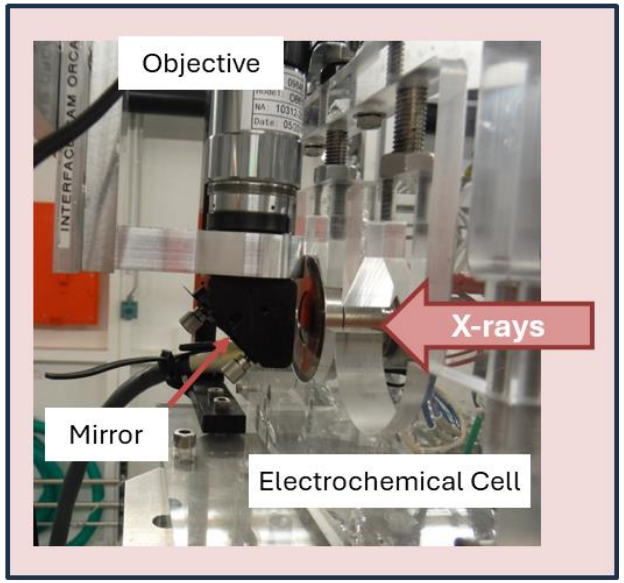

Field of View

3.3 mm x 1.2 mm (Navitar x4)

1.3 mm x 0,5 mm (Mitutuyo x10)

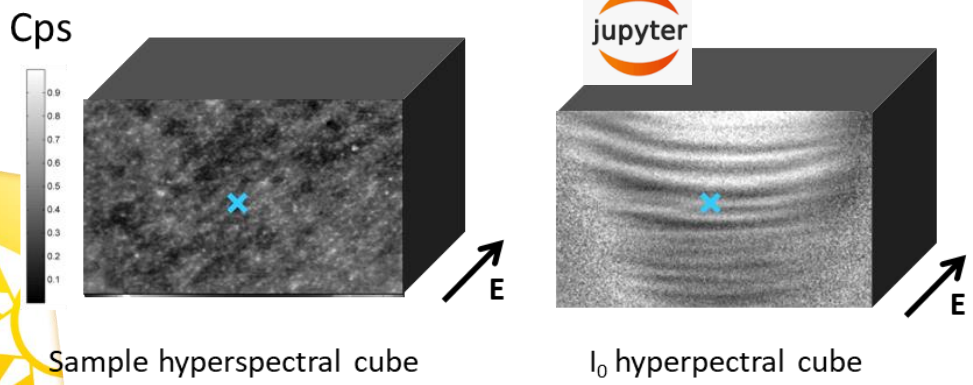

$\log(I_0/I)$

Spectrum on
1 single pixel
1 single cube

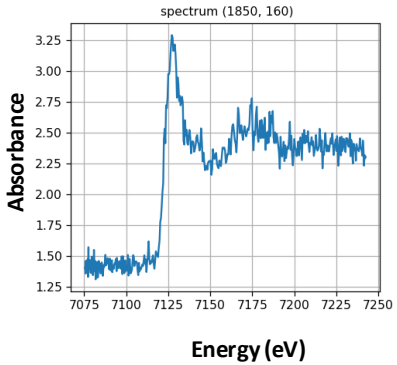

Spatial Resolution
3 – 4 µm

Time/cube
2 s (XANES)
4 to 11 s (XANES + EXAFS)

Briois *et al.*, *J. Sync. Rad.*, 2024, **31**, 1084-1104

$LiFePO_4$ Cycling with time- and spatially- resolved imaging

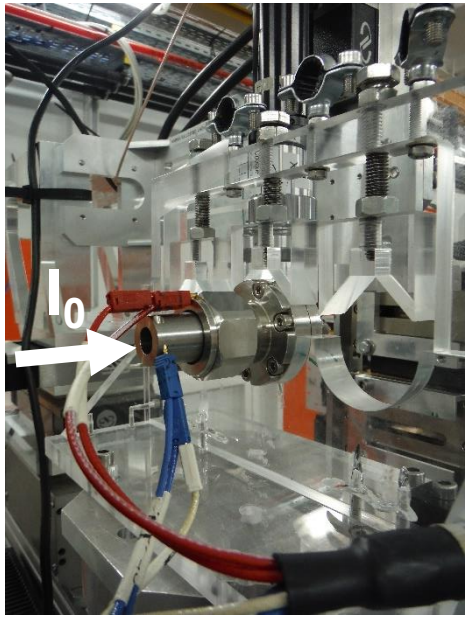

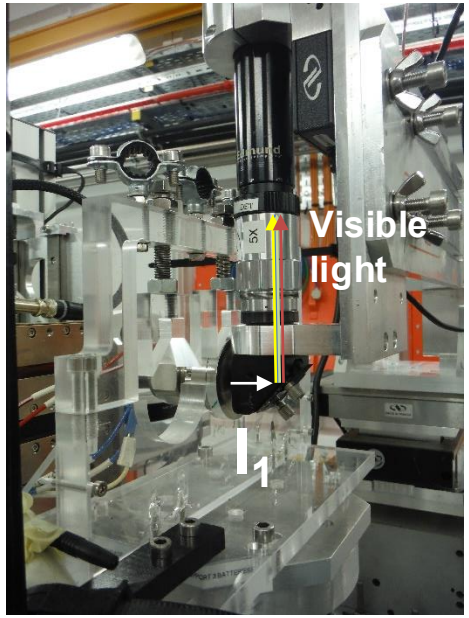

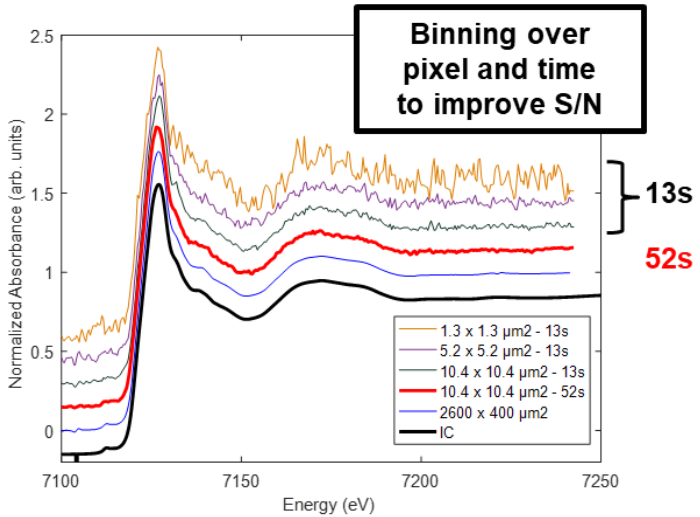

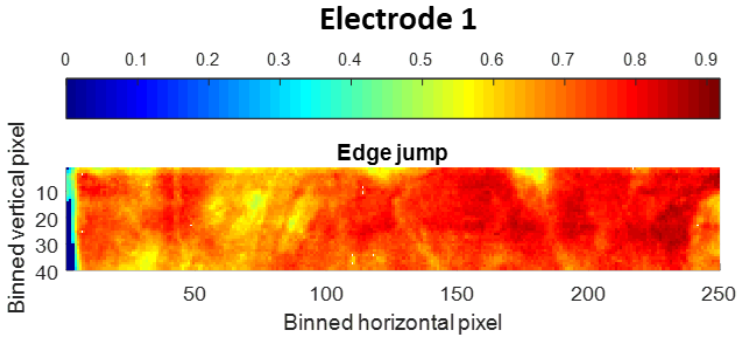

~ homogeneous distribution of Fe within the electrode

SPATIAL RESOUTION

ROI : 2048 (H) x 348 (V) pixels
Field of View : 2.66 (H) x 0.45 (V) mm^2
8x8 Pixel-binning : 10.4 x 10.4 μm^2

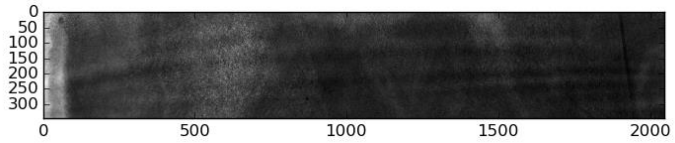

10200 (255 x 40) pixels/spectra per Cube after Pixel-Binning

Electrode Φ 6 mm

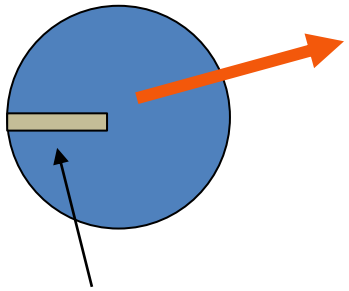

TIME RESOLUTION

Monitoring of 1C charge
1 cube every 13 s => -0,0036 Li

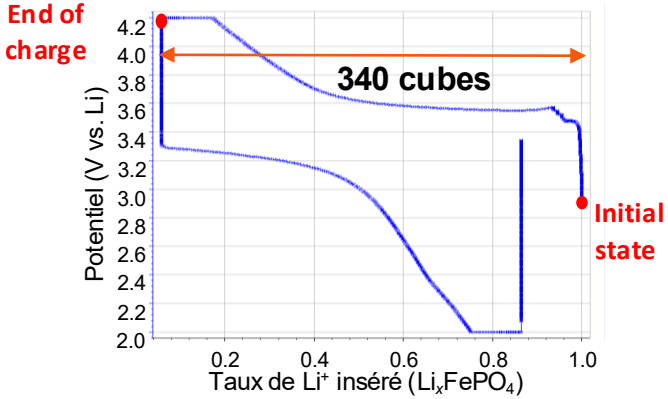

10200 pixels x 340 cubes
= **3 468 000 Spectra**

Briois *et al.*, *J. Sync. Rad.*, 2024, **31**, 1084-1104

Time and spatially- resolved imaging: A challenge for data processing

20000 spectra from flattened cube 1 + cube 340 (no-cube binning / 8 x 8 binned pixels)

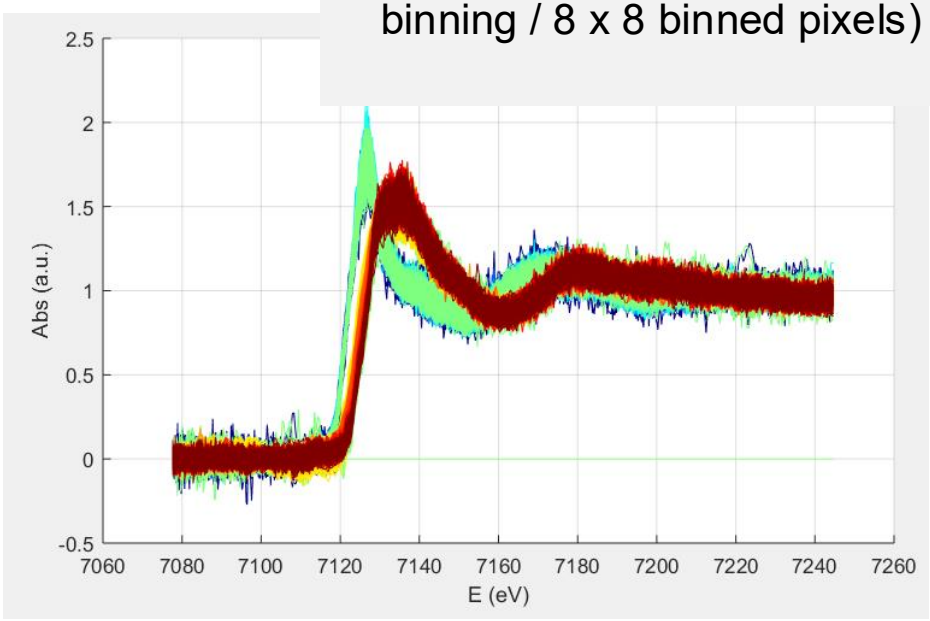

Cube 340

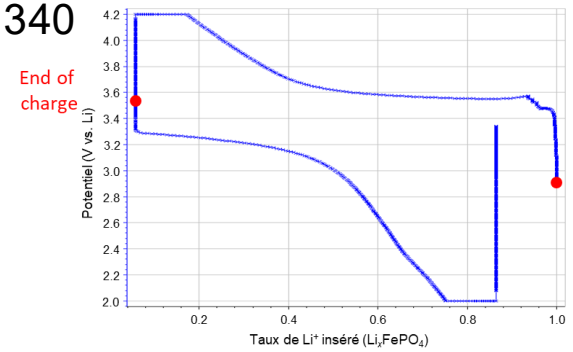

Cube 1

Initial state

MCR-ALS

$$D = CS^T + E$$

Constraints Used : Non negativity C and S^T + Closure relation

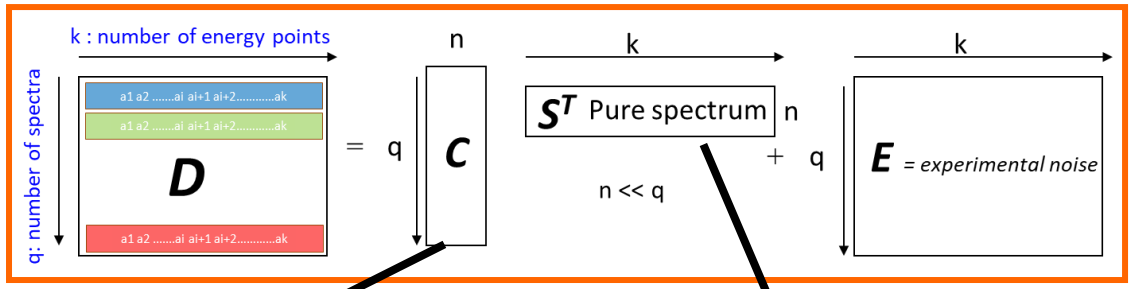

C

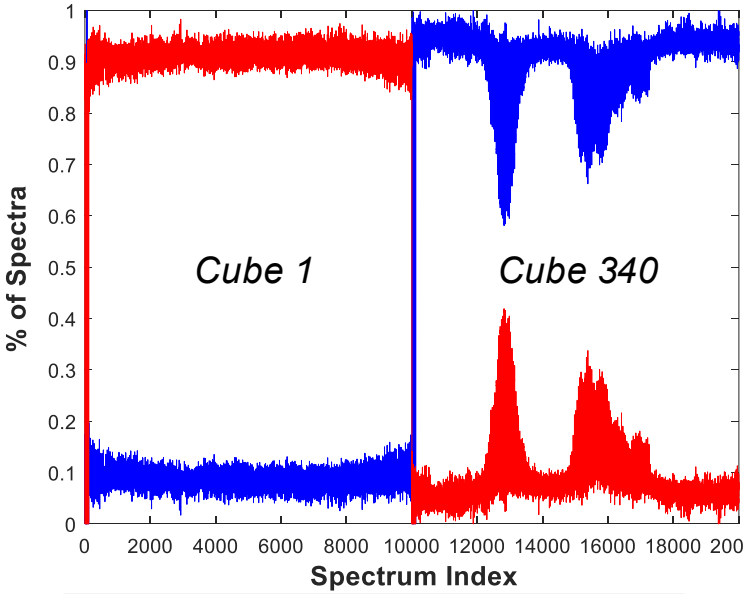

S^T

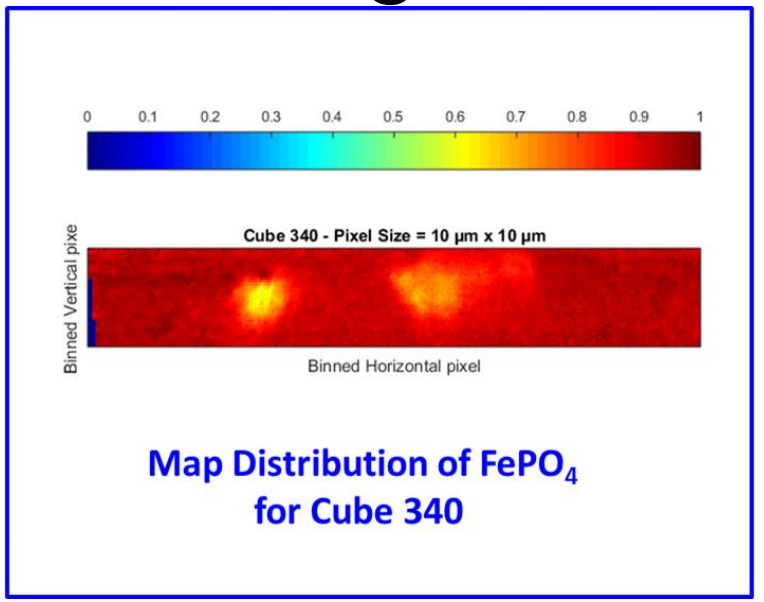

Briois *et al.*, *J. Sync. Rad.*, 2024, **31**, 1084-1104

Field of View : 2.66 (H) x 0.45 (V) mm^2

$LiFePO_4$ Cycling with time- and spatially- resolved imaging

Electrode Φ 6 mm

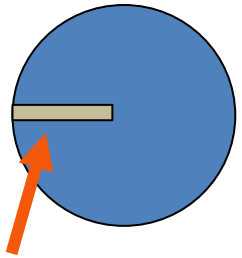

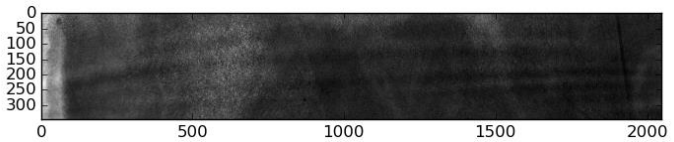

SPATIAL RESOUTION

ROI : 348 (H) x 2048 (V) pixels
8x8 Binning Pixel : 10.4 x 10.4 µm²
Field of View : 2.66 (H) x 0.45 (V) mm²

TIME RESOLUTION

Monitoring of 1C charge
1 cube every 13 s => -0,0036 Li

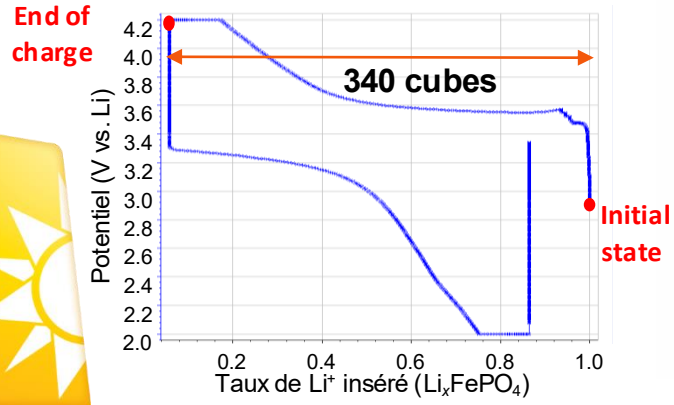

Use of Pure Species Spectra

for rebuilding by MCR-ALS the Speciation of Cubes at different stages of the charge
But with SELECTIVITY constraints

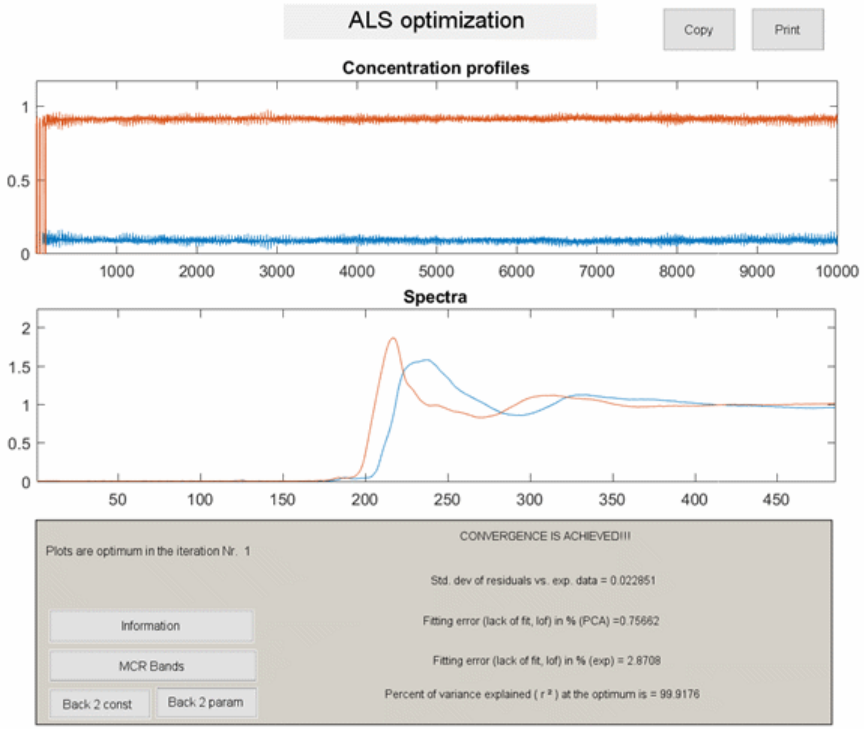

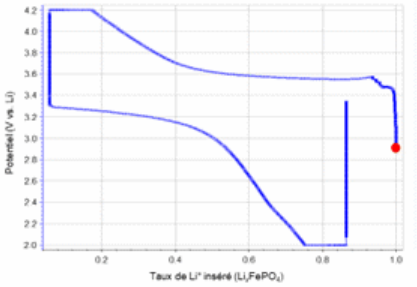

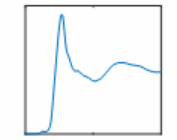

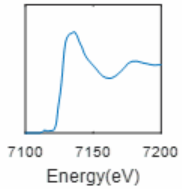

1C

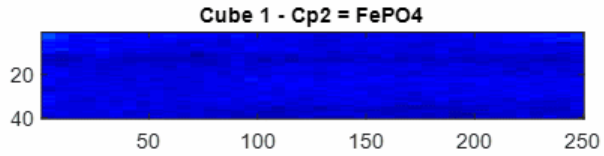

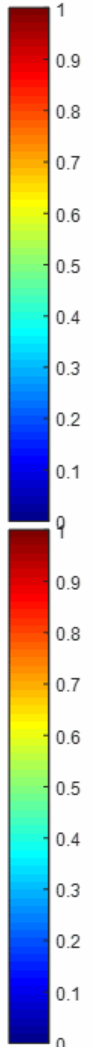

MCR-ALS on flattened spectra

FoV: 2.66 (H) x 0.45 (V) mm²

Briois *et al.*, *J. Sync. Rad.*, 2024, **31**, 1084-1104

$LiFePO_4$ Cycling with time- and spatially- resolved imaging

De-intercalation of 0.5 Li^+

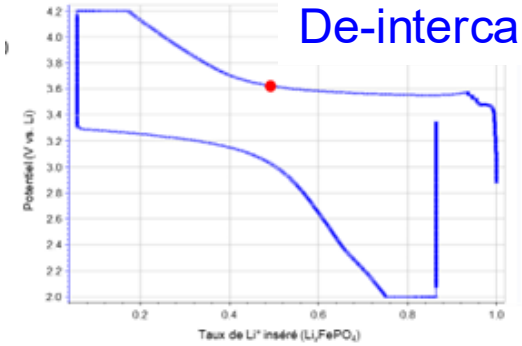

~ homogeneous distribution of Fe within the electrode

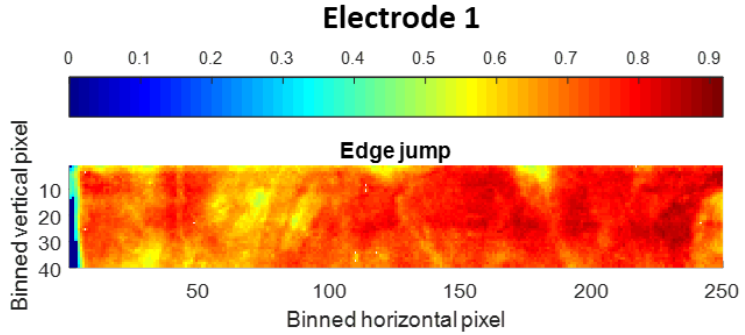

FoV: 2.66 (H) x 0.45 (V) mm^2

Electrode 2

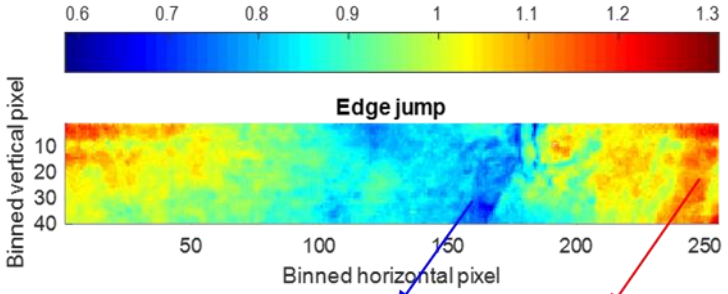

NON - homogeneous distribution of Fe within Electrode 2

Thin area

Thick area

LFP Fraction

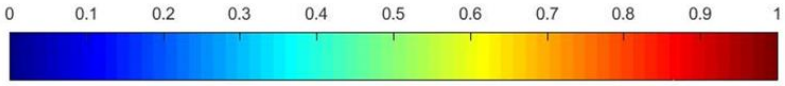

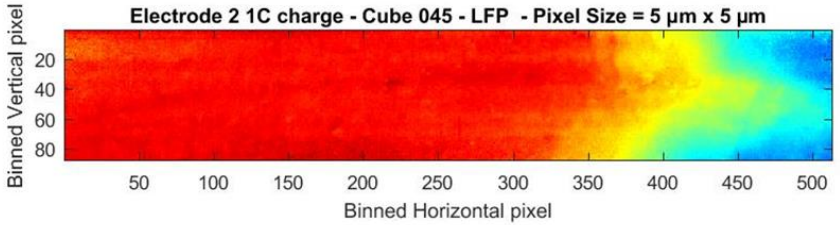

5.2 x 5.2 µm
2D spatial resolution
13 s/scan

1C

LFP Fraction

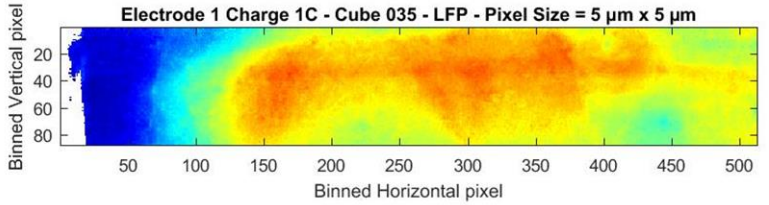

Electrode 1

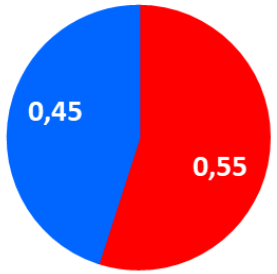

Electrode 2

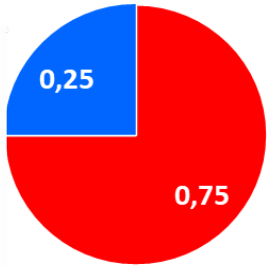

LFP FP

we are not so far from the composition
0.5 $FePO_4$ - 0.5 $LiFePO_4$
But with strong spatial heterogeneity

$LiFePO_4$ Cycling with time- and spatially- resolved imaging

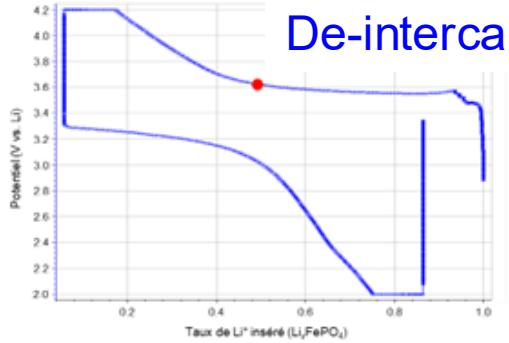

De-intercalation of 0.5 Li^+

~ homogeneous distribution of Fe within the electrode

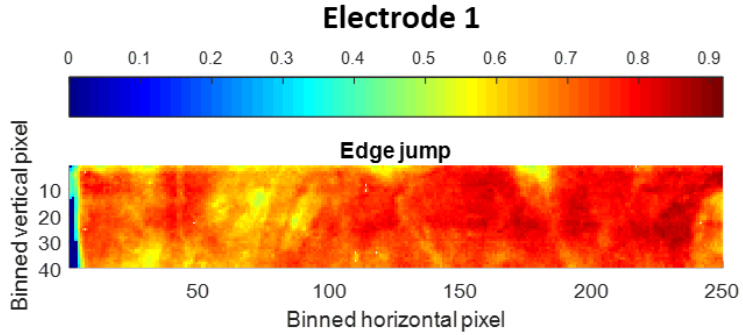

Quantifying Reaction and Rate Heterogeneity in Battery Electrodes in 3D through Operando X-ray Diffraction Computed Tomography

Hao Liu,[†,▽] Saeed Kazemiabnavi,[‡] Antonin Grenier,[†] Gavin Vaughan,[§] Marco Di Michiel,[§] Bryant J. Polzin,[∥] Katsuyo Thornton,[⊥] Karena W. Chapman,[*,†,#] and Peter J. Chupas[*,#,¶]

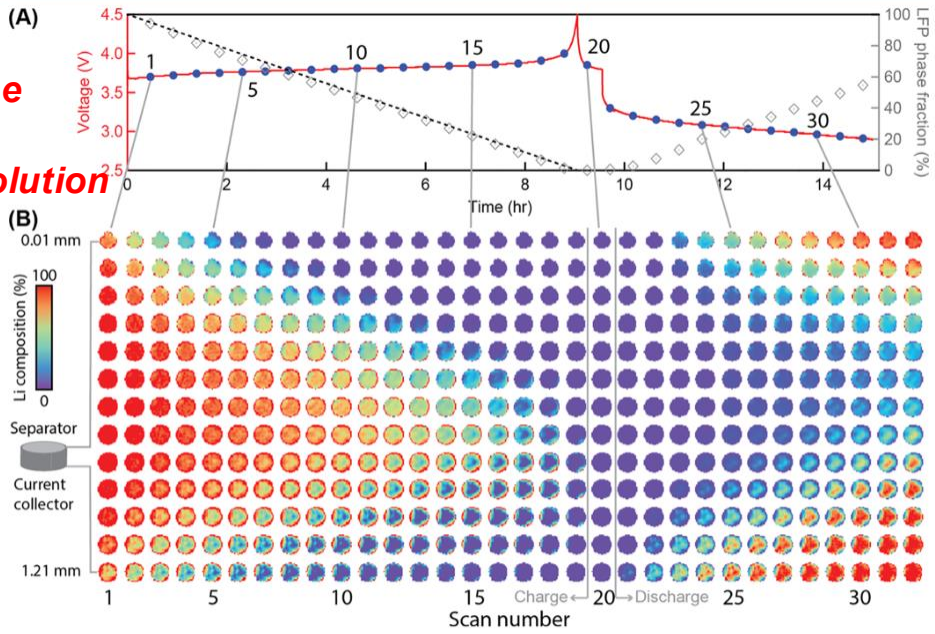

Figure 2. (A) Voltage profile of the thick electrode cycled at C/10 during operando XRD-CT (red curve). Blue dots indicate the time of each tomography measurement. Gray squares indicate the average LFP phase fraction of the entire electrode. The dashed black line indicates the ideal LFP phase fraction during galvanostatic charge. (B) LFP phase fraction, that is, the Li composition, map of different horizontal layers across the electrode during cycling. The Li composition (LFP phase fraction) is represented in color. The separation between adjacent layers is 0.1 mm.

ACS Appl. Mater. Interfaces 2019, 11, 18386−18394

200 µm in plane
100 µm depth
3D spatial resolution

30 min /scan

C/10

1C

5.2 x 5.2 µm
2D spatial resolution
13 s/scan

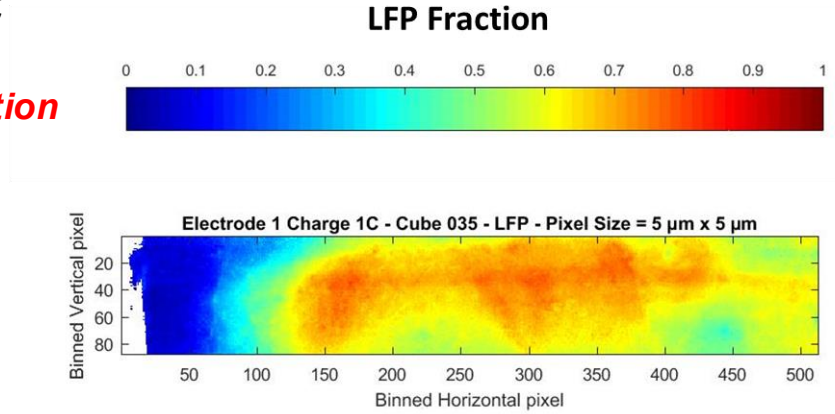

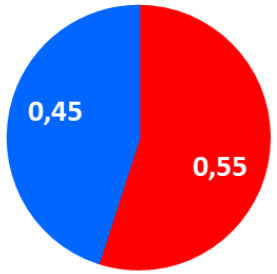

LFP FP

we are not so far from the composition
0.5 $FePO_4$ - 0.5 $LiFePO_4$
But with strong spatial heterogeneity

Some Advantages of FF imaging *vs* « classical Quick-EXAFS »

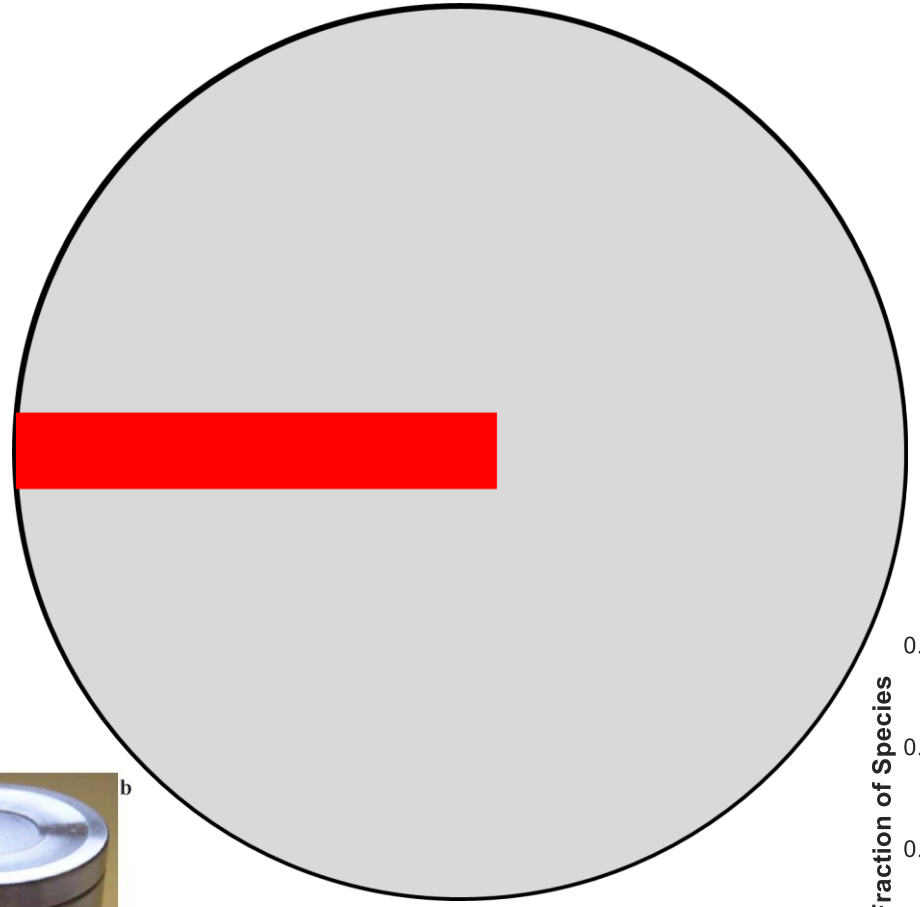

Electrode Φ 6 mm

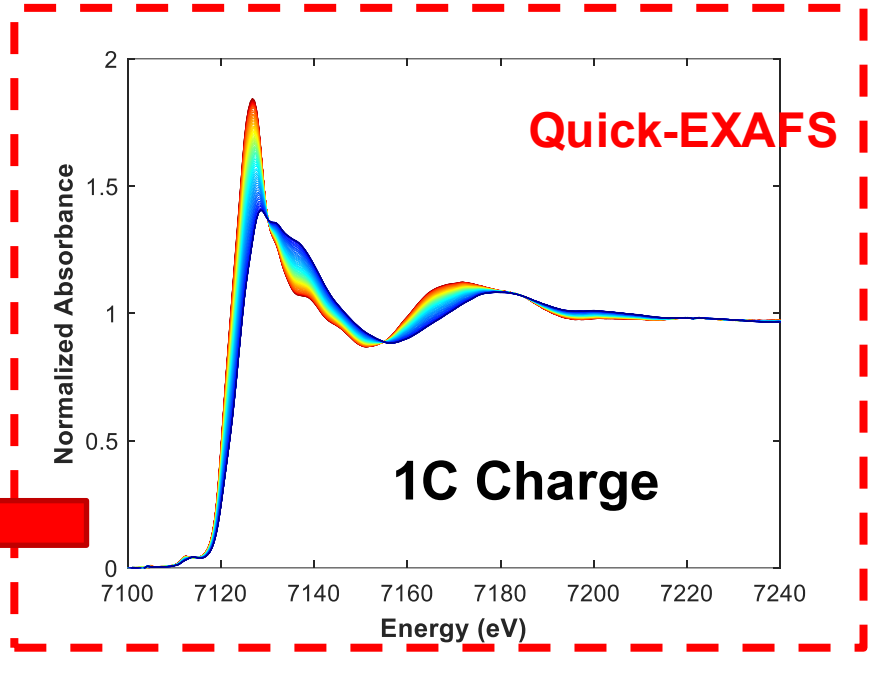

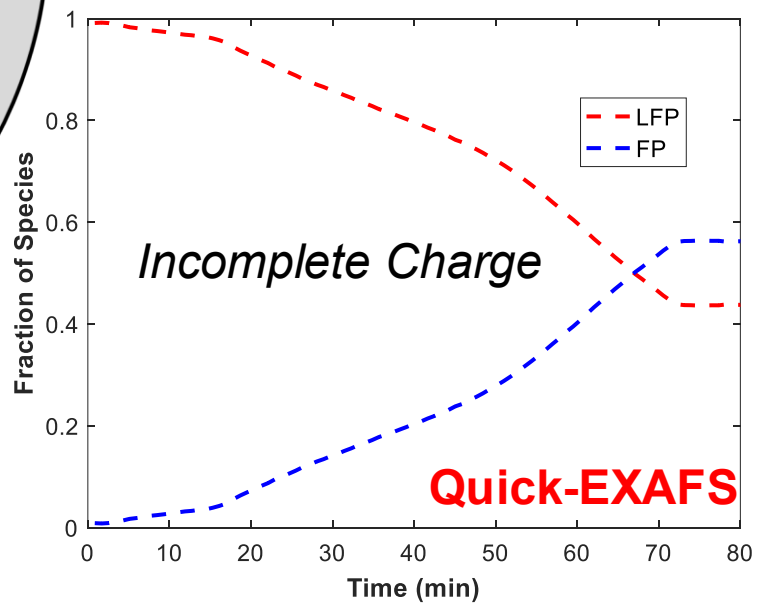

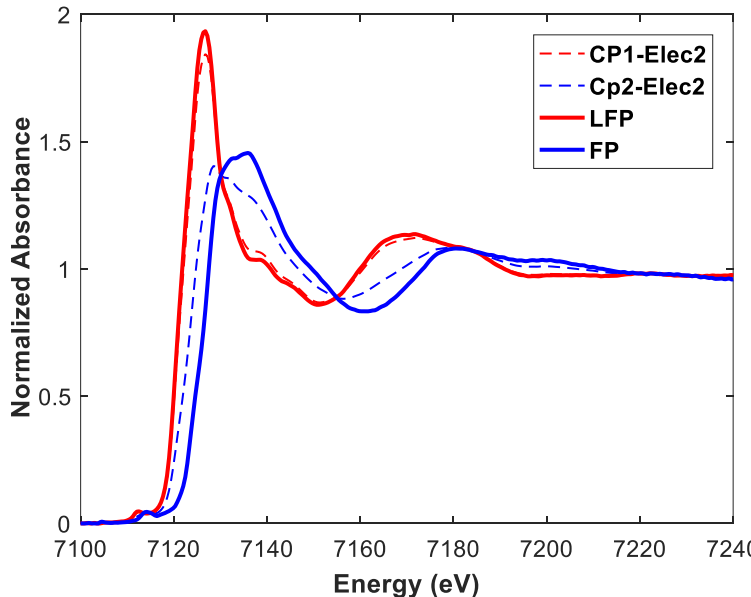

Some Advantages of FF imaging *vs* « classical Quick-EXAFS »

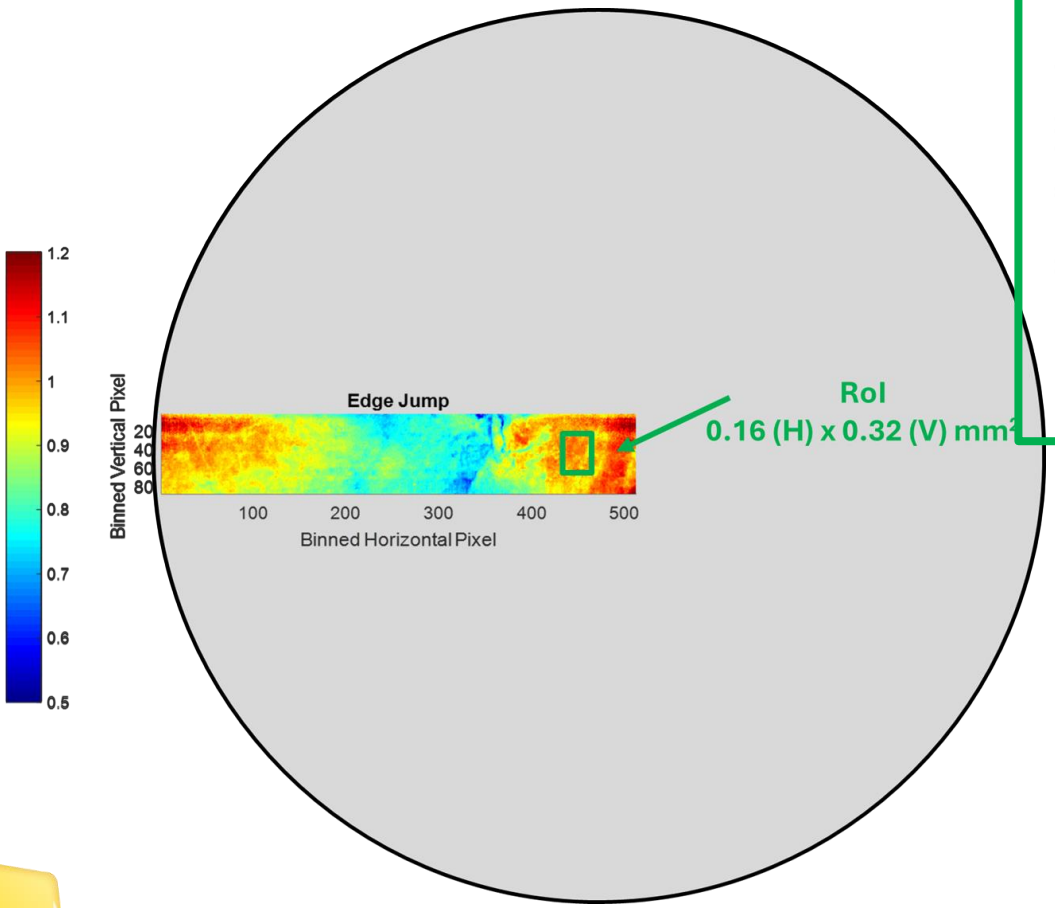

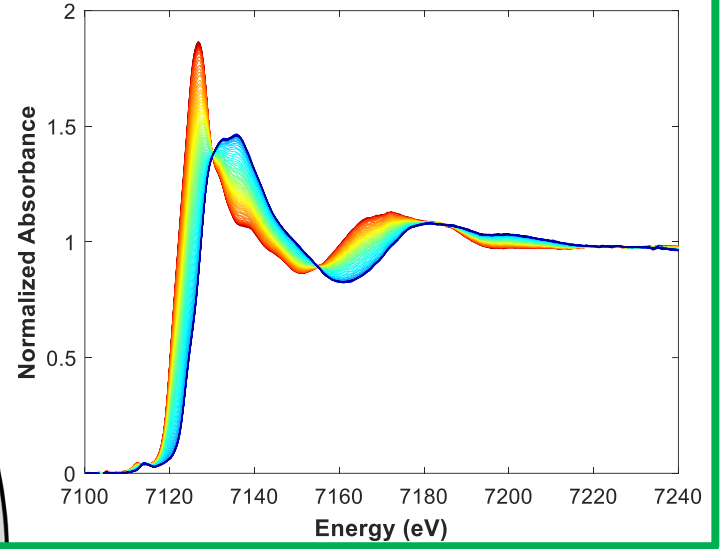

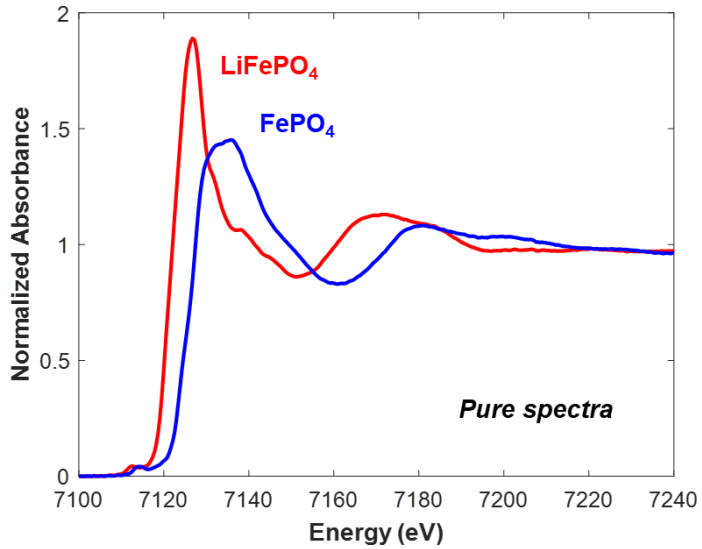

Looking inside the cell by hyperspectral imaging allows for drawing correct conclusions from the operando experiment

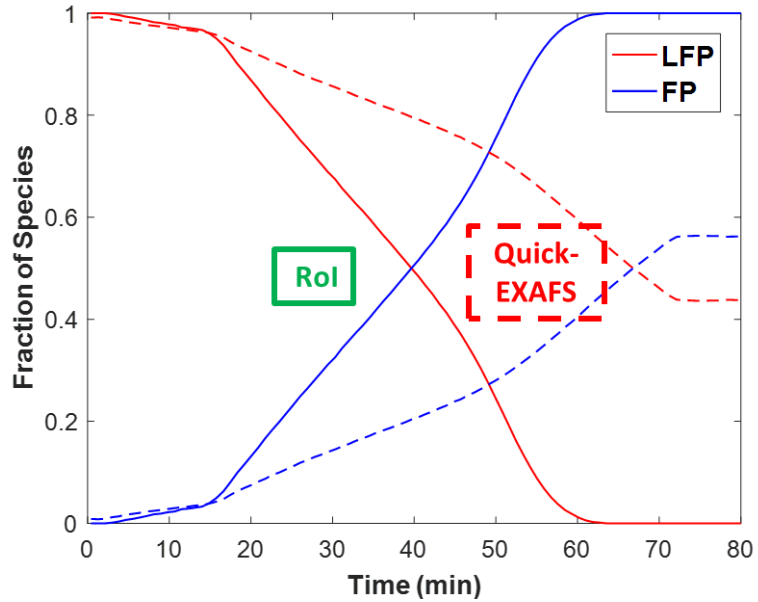

Some Advantages of FF imaging *vs* « classical Quick-EXAFS »

- With a larger beam = > decrease of beam damage

analytical chemistry

pubs.acs.org/ac Article

Are Operando Measurements of Rechargeable Batteries Always Reliable? An Example of Beam Effect with a Mg Battery

Lucie Blondeau, Suzy Surblé, Eddy Foy, Hicham Khodja, Stéphanie Belin,* and Magali Gauthier*

Cite This: *Anal. Chem.* 2022, 94, 9683–9689 Read Online

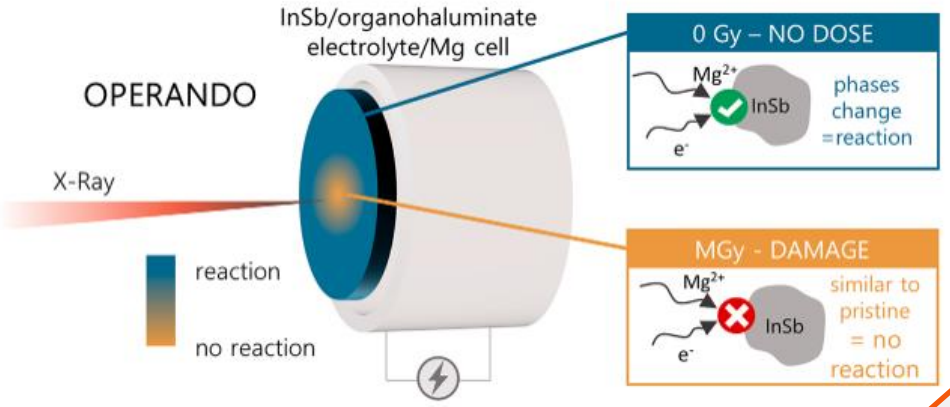

Beam size :
0.68 (H) x 0.28 (V) mm²

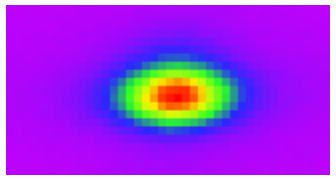

X 20: Dose decrease

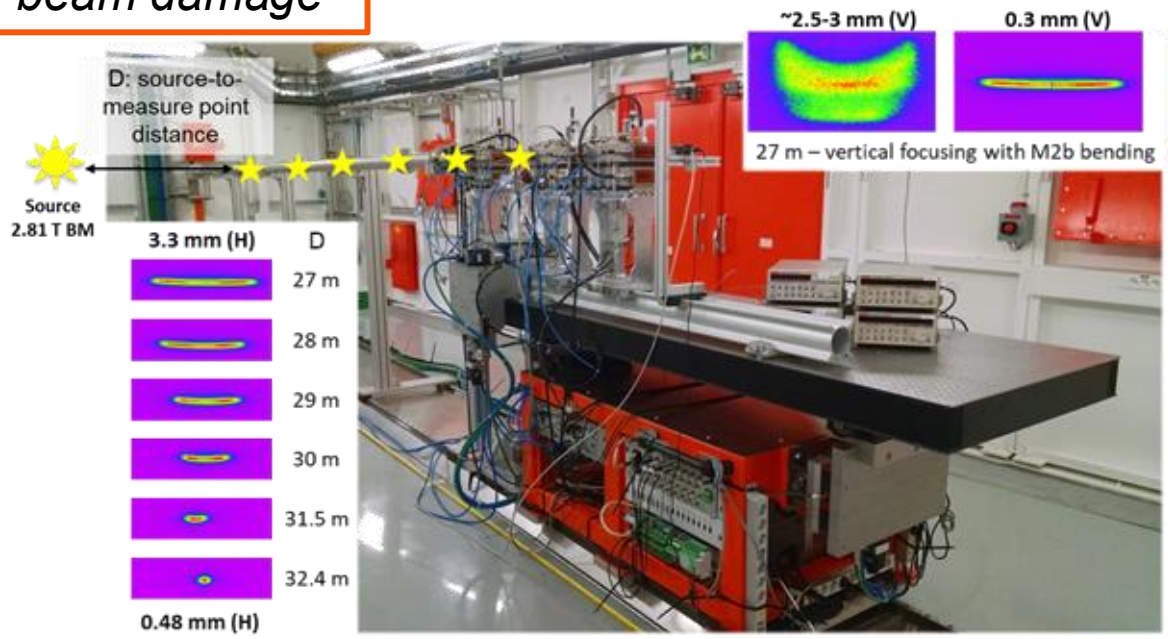

Field of View :
3,28 (H) x 1.21 (V) mm²

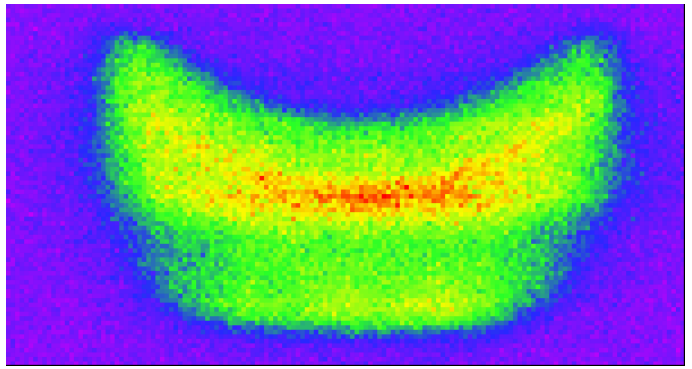

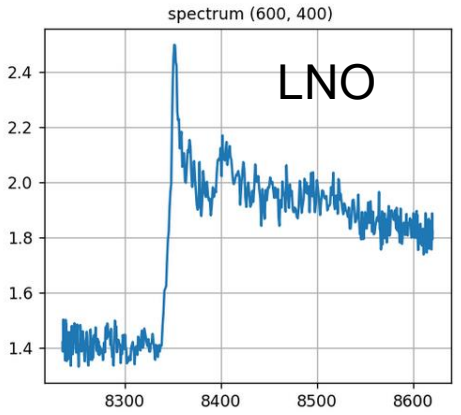

Noisier data but so many => MCR-ALS

X-ray Absorption Spectroscopy

LOCAL PROBE

- Atomic Selectivity
- All kind of materials
- Simplicity of data Collection
- Reaction Process

Which allows for

- direct determination of interatomic distances

- determination of electronic structure - Orbital Selectivity

Limitation :

- Not an absolute technique

- High sensitivity to the bulk

XAS is Element Specific

(from S. Webb)

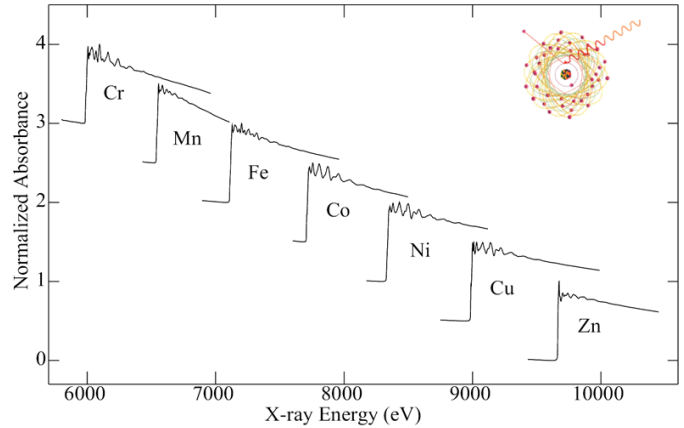

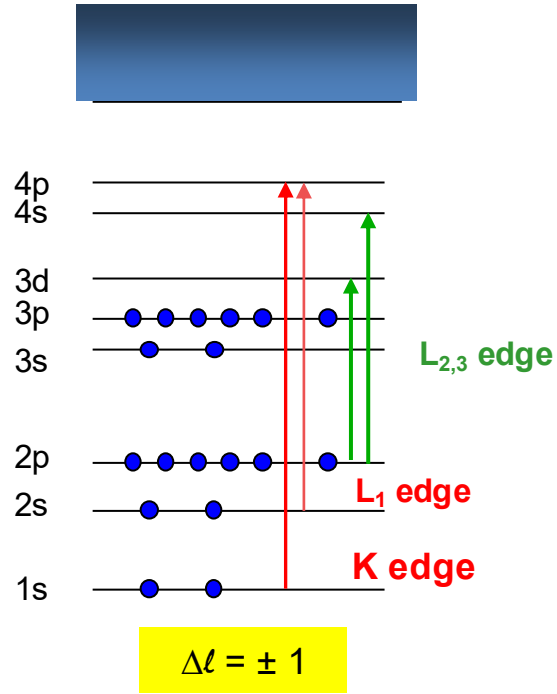

ROCK a beamline optimized for Operando characterizations

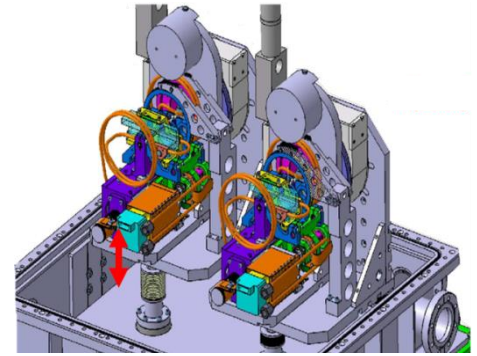

- ✓ **Time resolution ranging from 20 ms to 5s**
- ✓ **+ Space Resolution at the micron-meter scale**
- ✓ **3 Quick-EXAFS monochromators for 4-43 keV energy range**
- ✓ **"Edge jumping" capability**

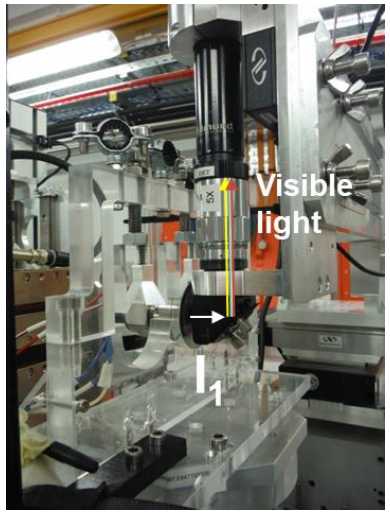

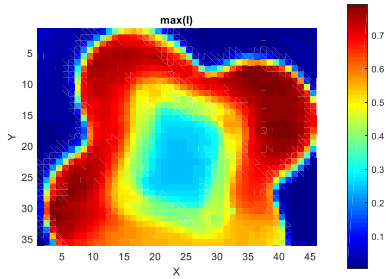

- ✓ **Dedicated sample environments for *operando* studies**

In energy storage, heterogeneous catalysis, electro-catalysis, photo-catalysis, nanoparticles nucleation/growth

- ✓ **Combination of Techniques**
  - **Raman spectroscopy**
  - **UV-Vis spectroscopy**
  - **2D microscopy**

- ✓ $D = C S^T + E$

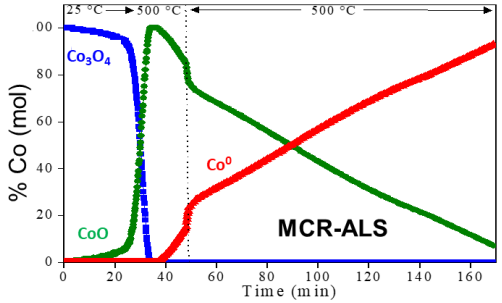

- ✓ **Modulation Excitation Spectroscopy**

$$A_k^{\phi^{PSD}}(e) = \frac{2}{T}\int_0^T A(e,t).\sin(k\omega t + \phi^{PSD}).\,dt$$

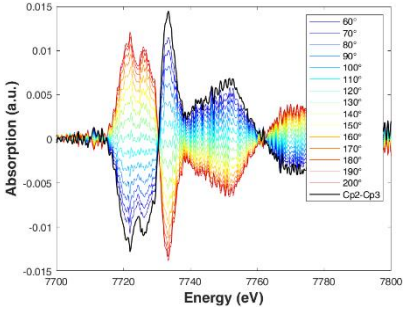

Synchrotron Radiation News (2020) 33(1) 20-25

Laurent Barthe

Stéphanie Belin

Anthony Beauvois

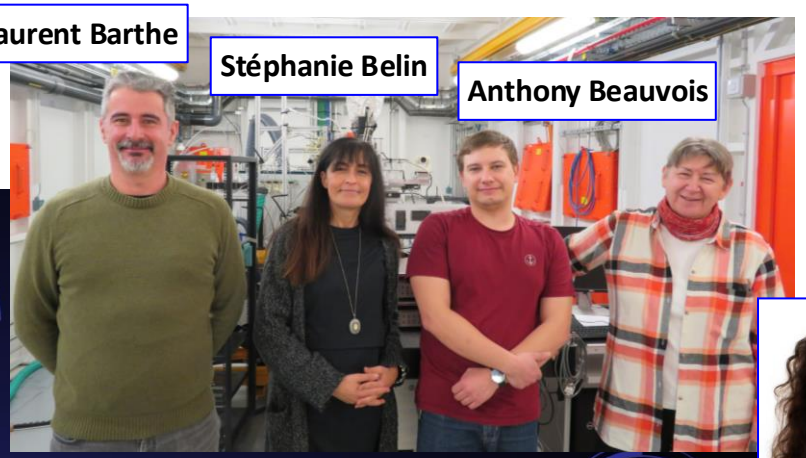

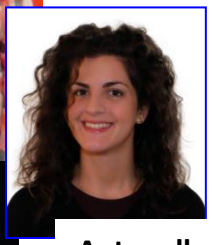

Antonella Iadecola (RS2E)

Beamlines supported by a Consortium for Catalysis and Energy-Related Materials

BIG-MAP

Gilles Moehl

Lucia Pérez Ramírez

Francesco La Porta

Olga Roudenko

Pionners of XAFS in France: Pierre Lagarde, Denis Raoux, Alain Fontaine, Dominique Chandesris, Georges Calas, Jacqueline Petiau, Michel Verdaguer, Françoise Villain, Christian Brouder

From LURE to SOLEIL : Michèle Sauvage, Jean Daillant

Pleanry Lectures : John Rehr, Yves Joly, Janis Timoshenko

Invited Lectures : Philippe Sainctavit, Christèle Legens, Sakura Pascarelli, Laurent Michot, Géraldine Sarret, Jean Susini, Laurence Croguennec, Karine Provost

Oral Communications will be selected on abstracts + Poste session

Ex Situ XAS study on LNO

Insights into the role of the covalent Ni–O bonds in $LiNiO_2$ positive electrodes: a correlative hard X-ray spectroscopy study

Jazer Jose H. Togonon, Jean-Noël Chotard, Alessandro Longo, Lorenzo Stievano, Laurence Croguennec and Antonella Iadecola

Representative NiO_2 layers composed of edge-sharing NiO_6 octahedra and a Li interlayer from the $LiNiO_2$ crystal structure, highlighting a local NiO_6 unit. A simplified band diagram illustrates the negative charge transfer from O 2p to Ni 3d states.

J. Mater. Chem. A, 2025, **13**, 28305-28317
https://doi.org/10.1039/D5TA03573B

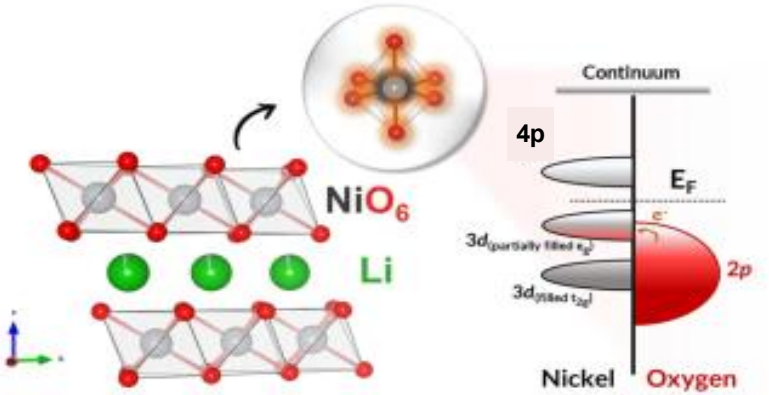

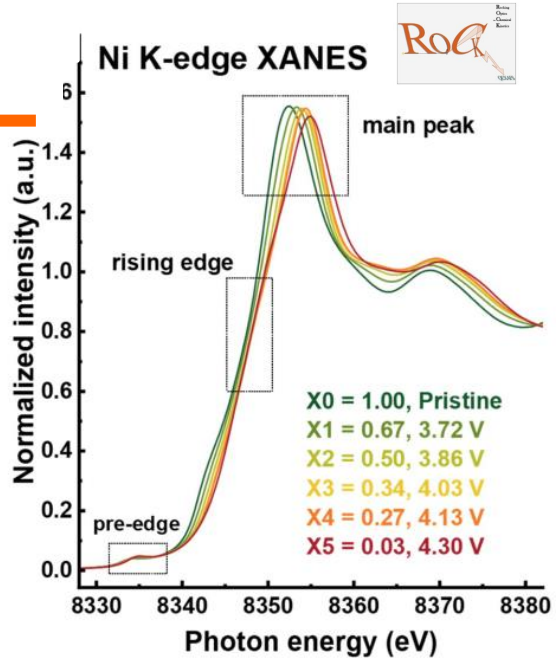

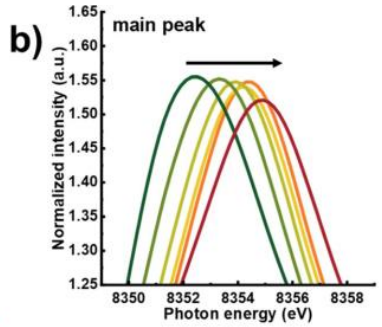

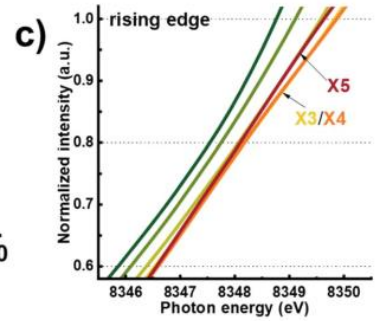

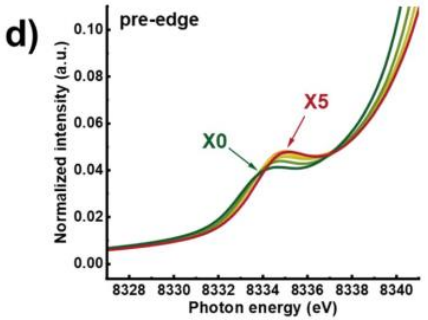

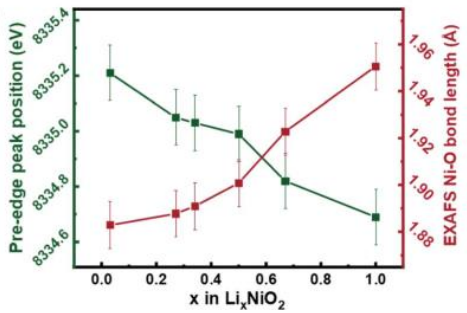

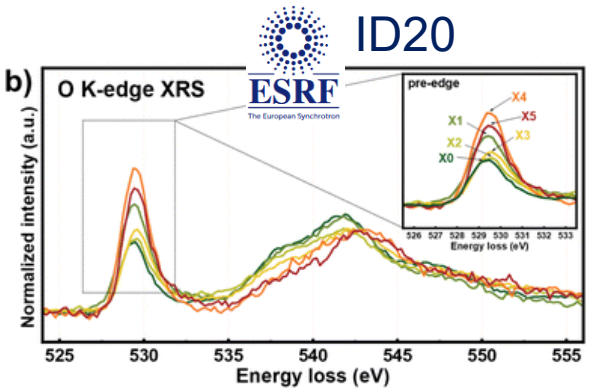

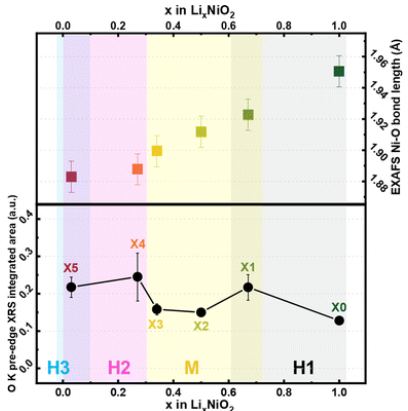

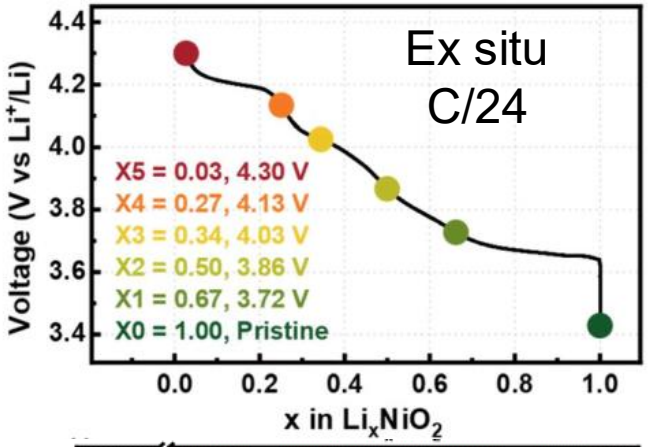

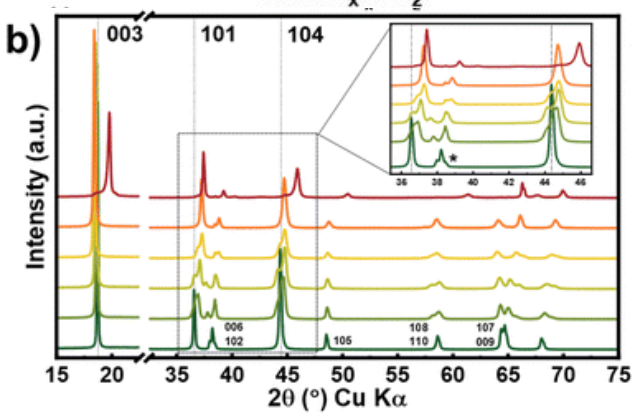

Sample - Formula	Crystal Phase from XRD	EXAFS $d_{(Ni-O)}$, Å
X0 - $LiNiO_2$	Hexagonal	1.95(1) × 6
X1 - $Li_{0.67}NiO_2$	Monoclinic	1.88(1) × 4 2.00(1) × 2
X2 - $Li_{0.50}NiO_2$	Monoclinic	1.87(1) × 4 1.99(1) × 2
X3 - $Li_{0.34}NiO_2$	Monoclinic	1.87(1) × 4 1.96(1) × 2
X4 - $Li_{0.27}NiO_2$	Hexagonal	1.89(1) × 6
X5 - $Li_{0.03}NiO_2$	Hexagonal	1.88(1) × 6

Co_3Mn-based LDH used as electro-chemical H_2O_2 sensor

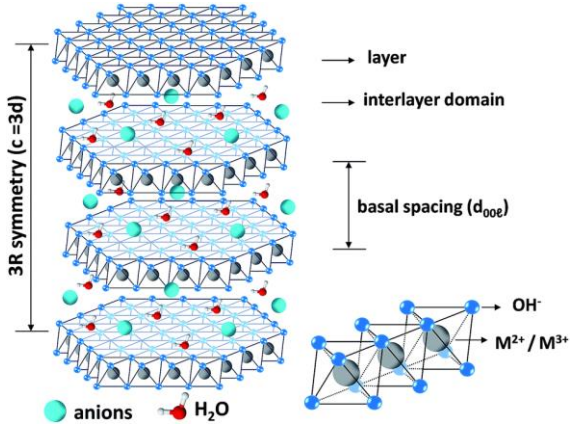

Santos et al., *J. Mater. Chem. A*, 2017, **5**, 9998

Operando X-ray Absorption Spectroscopy of $Co_3Mn–CO_3$ LDH: Formation and Structural Evolution under Electrochemical Conditions

Hani Farhat, Christine Mousty, Vanessa Prevot, Anthony Beauvois, Stéphanie Belin, Valérie Briois,* and Claude Forano*

Cite This: *J. Phys. Chem. C* 2024, 128, 21023–21037 Read Online

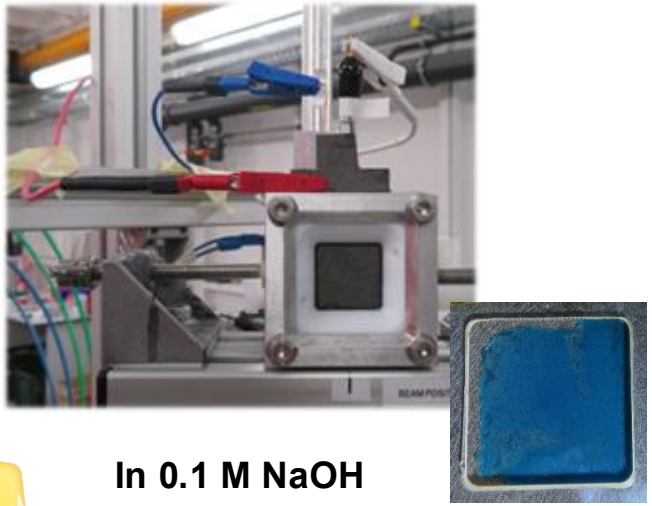

In 0.1 M NaOH

Carbon paper for material deposition

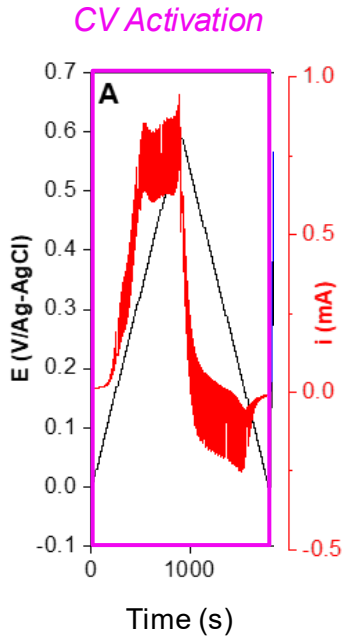

Transformation during electro-chemical CV activation

$Co(II)_3Mn(III)$ LDH → **$Co(III)_3Mn(IV)$ Layered Species**

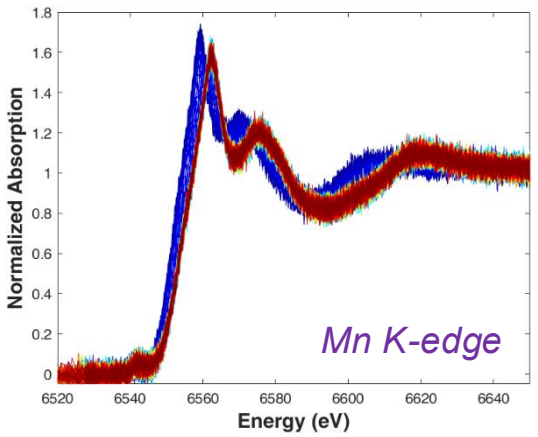

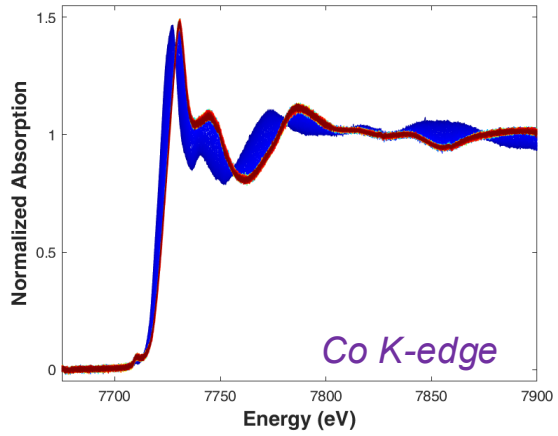

INSTITUT DE CHIMIE DE CLERMONT-FERRAND

Co_3Mn-based LDH used as electro-chemical H_2O_2 sensor

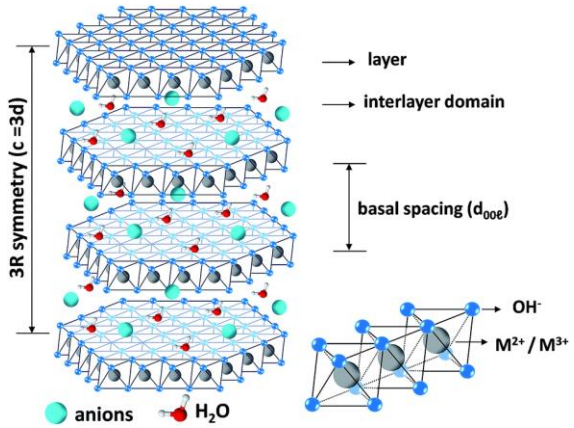

Santos et al., *J. Mater. Chem. A*, 2017, **5**, 9998

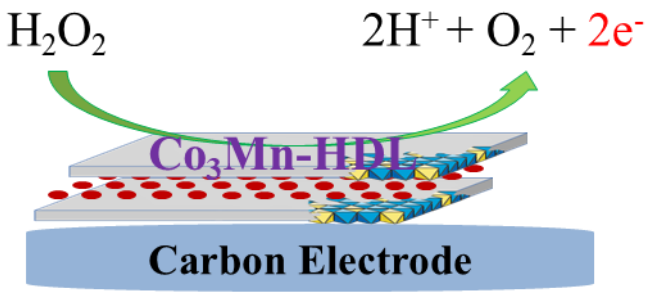

Farhat et al., *J. Phys. Chem. C*, 2020, **124**, 15585−15599

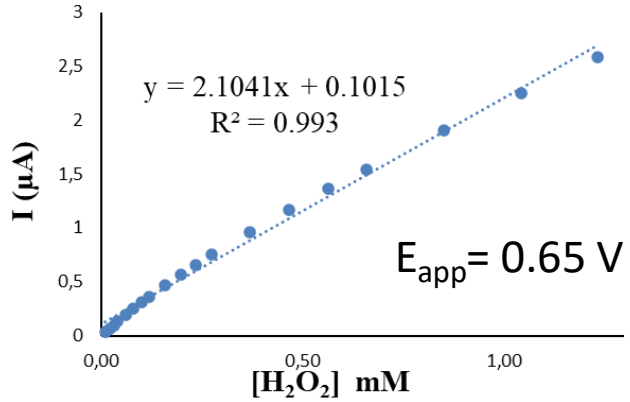

Operando : Activated Catalyst + H_2O_2

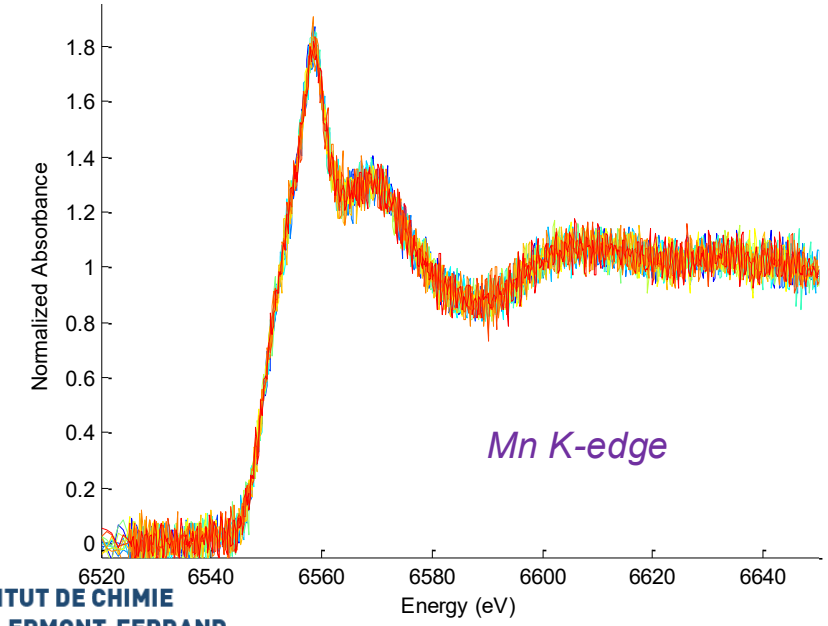

XAS is a bulk technique and electro-catalysis proceeds at the interface liquid-electrode.

How to increase the interface sensitivity?

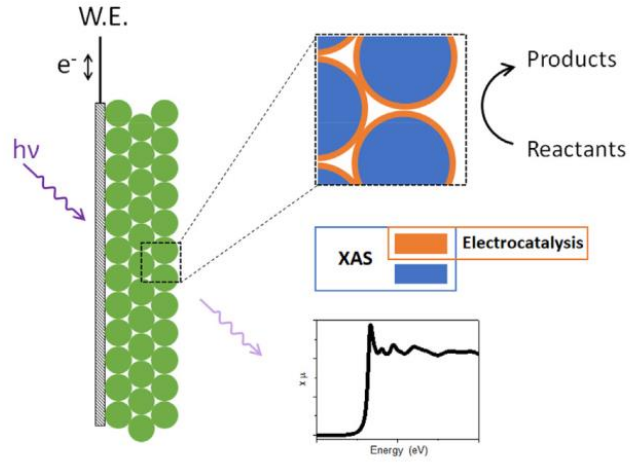

Current Opinion in Electrochemistry 2021, **27**:100681

INSTITUT DE CHIMIE DE CLERMONT-FERRAND

Modulation excitation XAS

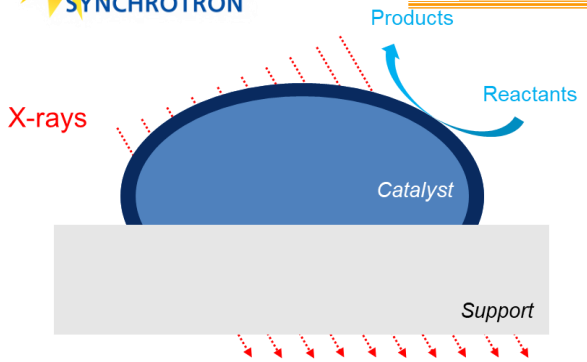

⇨ X-ray Absorption Spectroscopy is a bulk technique

What is seen by XAS *What we need to see*

? How to extract the reactive species when they are not the major part of the material of interest?

1. Applying a periodic stimuli to the system

2. Average the periods when the steady state is reached

3. Apply Phase-Sensitive Detection

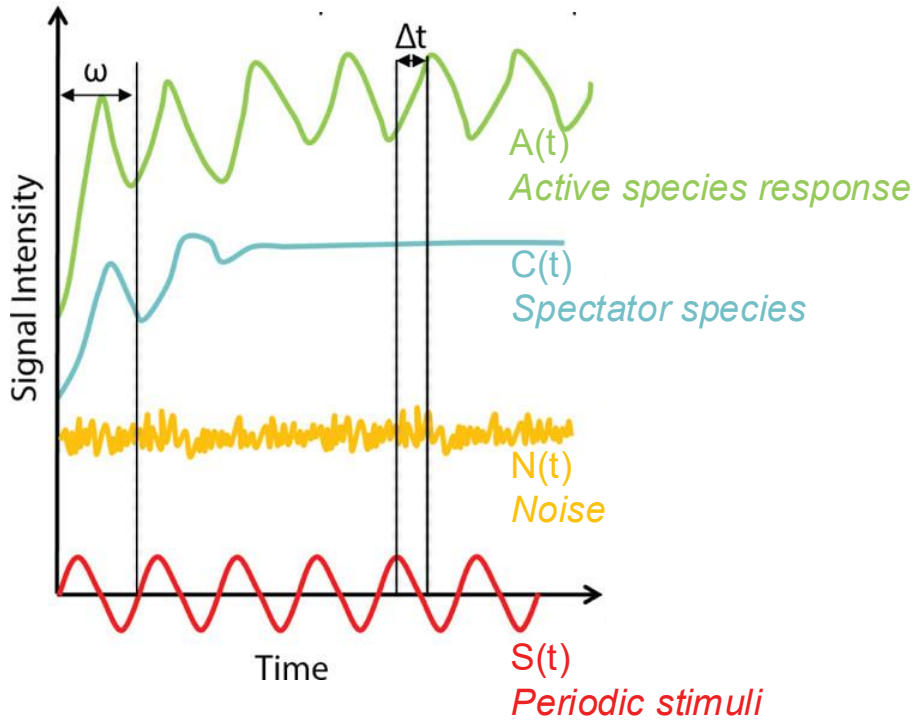

PSD

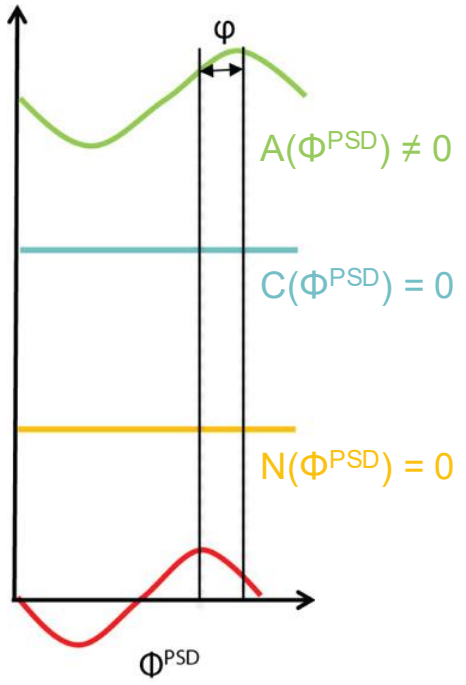

$$A_k^{\phi^{PSD}}(e) = \frac{2}{T}\int_0^T A(e,t).\sin(k\omega t + \phi^{PSD})\,.\,\mathrm{d}t$$

Müller et al., *Ind. Eng. Chem. Res.* 2017, **56**, 1123−1136; Urakawa et al., *Chem. Eng. Sc.,* 20, **63**, 4902-4909

Co_3Mn-based LDH used as electro-chemical H_2O_2 sensor

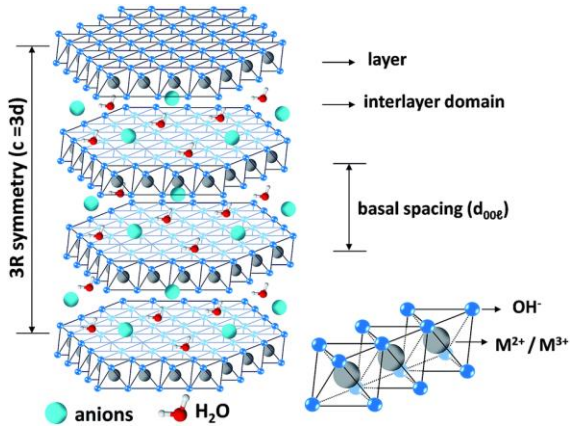

Santos et al., *J. Mater. Chem. A*, 2017, **5**, 9998

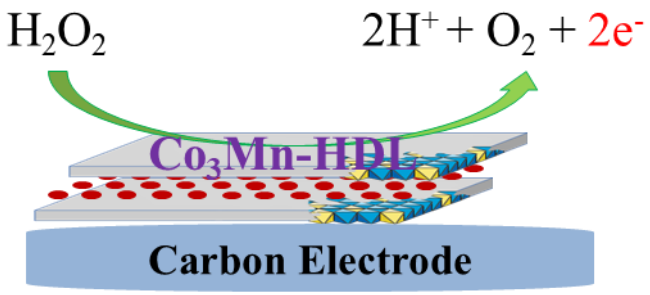

Farhat et al., *J. Phys. Chem. C*, 2020, **124**, 15585−15599

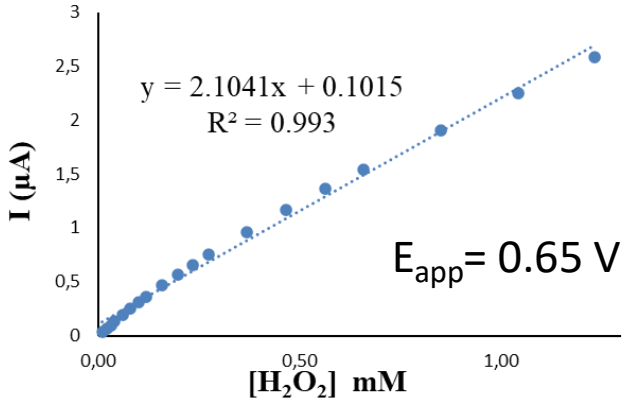

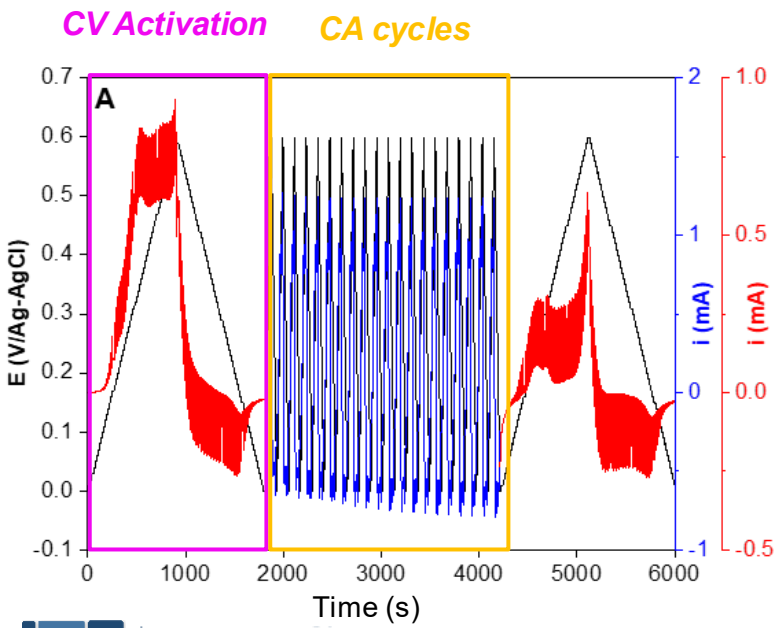

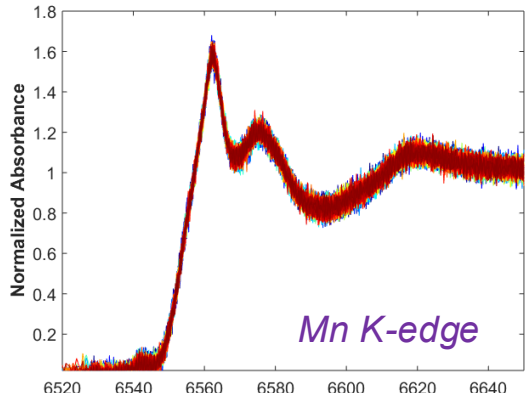

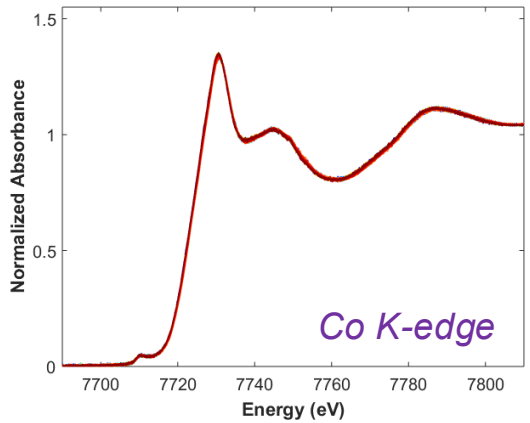

Which element is responsible for the electrochemical response of Co_3Mn LDH?

Is their synergic effect between Co and Mn?

INSTITUT DE CHIMIE DE CLERMONT-FERRAND

Electrochemical behaviour of Co_3Mn LDH

Electrochemical treatment : CA pulses

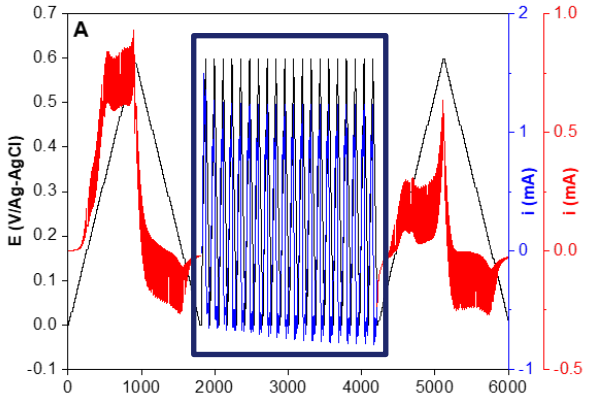

Focus on CV reversible pulses

1. Average the spectra into 1 period

2. Apply Phase Sensitive Detection (PSD)

$$A_k^{\phi^{PSD}}(e) = \frac{2}{T}\int_0^T A(e,t).\sin(k\omega t + \phi^{PSD}).\mathrm{d}t$$

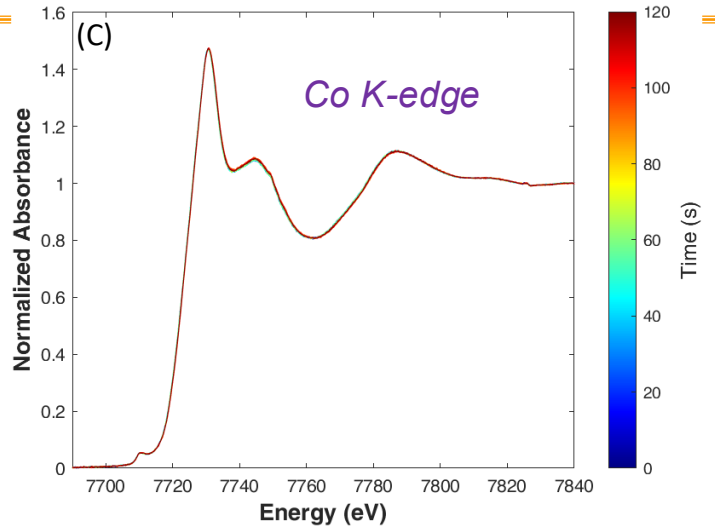

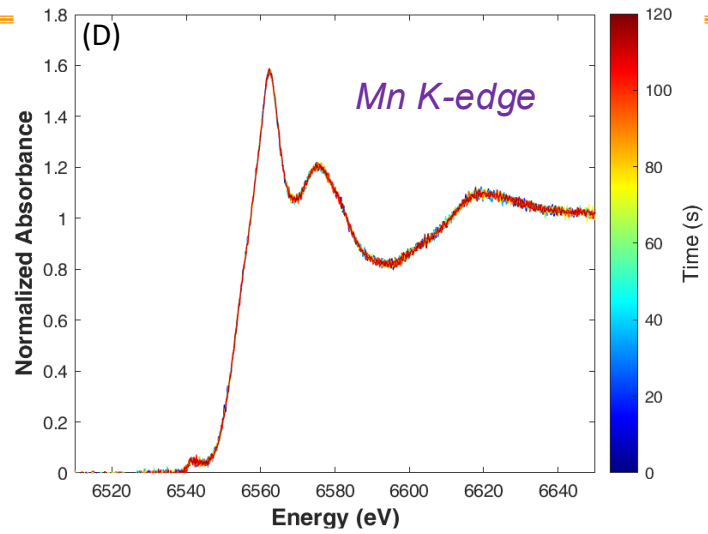

PSD

Only the Co is sensitive to CV pulses
2 Co species involved

PSD

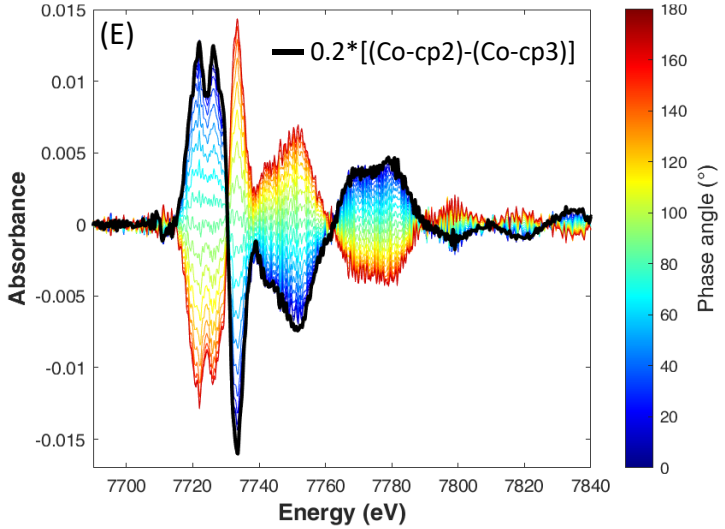

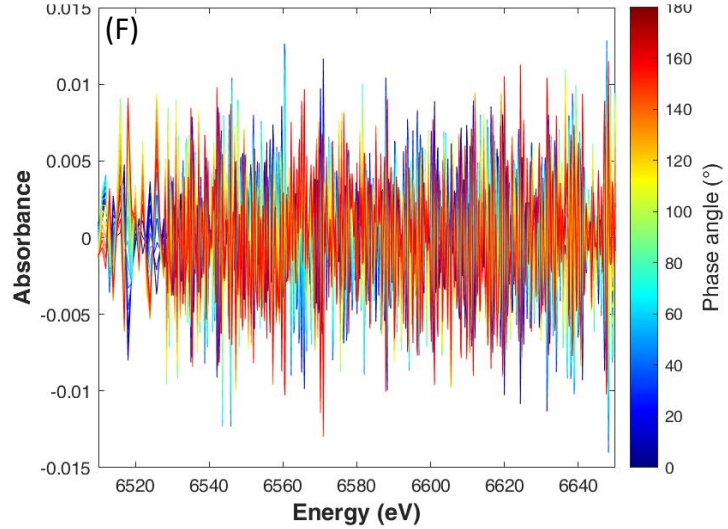

https://doi.org/10.1021/acs.jpcc.4c03883
J. Phys. Chem. C 2024, 128, 21023−21037